

Dissipative dynamics of an open quantum battery in the BTZ spacetime

Zehua Tian,^{1a} Xiaobao Liu,^b Jieci Wang,^c Jiliang Jing^c

^a*School of Physics, Hangzhou Normal University, Hangzhou, Zhejiang 311121, China*

^b*Department of physics and electrical engineering, Liupanshui Normal University, Liupanshui 553004, Guizhou, China*

^c*Department of Physics, Key Laboratory of Low Dimensional Quantum Structures and Quantum Control of Ministry of Education, and Synergetic Innovation Center for Quantum Effects and Applications, Hunan Normal University, Changsha, Hunan 410081, China*

E-mail: tzh@hznu.edu.cn, xiaobaoliu@hotmail.com, jcwang@hunnu.edu.cn,
jljing@hunnu.edu.cn

ABSTRACT: We consider how charging performances of a quantum battery, modeled as a two-level system, are influenced by the presence of vacuum fluctuations of a quantum field satisfying the Dirichlet, transparent, and Neumann boundary conditions in the BTZ spacetime. The quantum battery is subjected to an external static driving which works as a charger. Meanwhile, the quantum field is assumed to be coupled to both longitudinal and transverse spin components of the quantum battery including decoherence and pure dephasing mechanisms. Charging and discharging dynamics of the quantum battery are derived by extending the previous open quantum system approach in the relativistic framework to this more general scenario including both the driving and multiple coupling. Analytic expressions for the time evolution of the energy stored are presented. We find that when the driving amplitude is stronger/weaker than the energy-level spacing of the quantum battery the pure dephasing dissipative coupling results in better/worse charging performances than the decoherence dissipative coupling case. We also find that higher Hawking temperature helps to improve the charging performance under certain conditions compared with the closed quantum battery case, implying the feasibility of energy extraction from vacuum fluctuations in curved spacetime via dissipation in charging protocol. Different boundary conditions for quantum field may lead to different charging performance. Furthermore, we also address the charging stability by monitoring the energy behaviour after the charging protocol has been switched off. Our study presents a general framework to investigate relaxation effects in curved spacetime, and reveals how spacetime properties and field boundary condition affect the charging process, which in turn may shed light on the exploration of the spacetime properties and thermodynamics via the charging protocol.

Keywords: BTZ spacetime, Quantum vacuum fluctuations, Quantum battery, Dissipation

¹Corresponding author, Email:tzh@hznu.edu.cn

Contents

1	Introduction	1
2	The model	3
2.1	Open quantum battery model	3
2.2	Charging performance indicators	6
3	Quantum battery in BTZ spacetime	7
3.1	Charging dynamics	9
3.2	Effect of dissipation on average energy	12
3.2.1	$\Delta < A$ case	12
3.2.2	$\Delta \geq A$ case	17
3.3	Direct comparison of $\langle E \rangle$ for different coupling form	21
3.4	Charging stability	22
4	Discussions and Conclusions	25

1 Introduction

In the era of quantum supremacy for quantum computing [1, 2], the so called “quantum thermodynamics” [3–6] has emerged to explore the thermodynamics concepts, such as work and heat, at the quantum scale, as well as to develop the new thermodynamic protocols exploiting quantum mechanical resources in the thermodynamic protocol, such as entanglement and coherence, to outperform their classical counterparts. A simple paradigm to explore this issue is a quantum battery (QB): a designed device operating in the quantum regime capable of temporarily storing energy for later use [7–9].

The notion of QB was first introduced in the seminal work [7] by Alicki and Fannes, showing entangling unitary controls extract in general more work than independent ones. Afterward, the development of different figures of merit, such as the charging time, the associated power, and the amount of extractable work, has been a major focus on the QB physics [9–16]. To improve the charging performance, a lot of methods have been developed to assist the charging protocol, including collective quantum resources [17–19], ordered and disordered interactions [20], external environment engineering [21–24], collisional model [25, 26], Sachdev-Ye-Kitaev model [27, 28] and so on; see Ref. [9] for an extensive review and a comprehensive list of references. Beyond the theoretical analysis, the experimental implementation of various kinds of QBs and different charging protocols has also been reported recently [9, 29–33]. Furthermore, since any systems are unavoidably coupled to the environment, at least subjected to vacuum fluctuations at the quantum scale, relaxation and dephasing would play a key role in the system dynamics. In this sense, the QB’s

figures of merit, including the maximum average energy stored during the charging protocol, the charging power, the charging stability and so on, inevitably undergoes the relaxation and dephasing, which may even dominate the QB charging performance. It is thus of great importance to learn the charging performance in the presence of inevitable external environmental action [9, 34–40].

On the other hand, open quantum system approach [41–43] has been extended to the relativistic framework by considering a two-level quantum system (or detector) coupled to vacuum fluctuations of quantum fields in different spacetimes and undergoing various relativistic motions [44–49]. Because of the quantum field scattering by spacetime, through the interaction between the detector and fields the information of spacetime properties and relativistic motions may be encoded into the dynamical evolution of the detector. Therefore, the open quantum system approach has been fruitfully applied in the relativistic framework to exploring various physics, such as understanding and detecting relativistic effects and spacetime properties [46, 47, 50–58], measuring quantum state and work distributions of quantum fields [59–61], and so on. Furthermore, this simple but effective detector-field model has been extensively utilized in the exploration of interplay between relativity and quantum mechanics [62–66].

In this paper, we extend the charging protocol of QB to the relativistic framework, trying to explore thermodynamics, relativity and the interplay with the laws of quantum mechanics jointly through dissipation dynamics. We therefore inspect the dynamics of a QB, modeled as a two-level atom. It is coupled to the vacuum fluctuations of quantum field in the BTZ spacetime responsible for dissipation, and meanwhile is operated by a static external classical driving acting as a charger. Note that the external driving on quantum system is essential to quantum state preparation, system manipulation and final state readout in the quantum information process [67–70]. To obtain the QB’s dynamics, we extend the previous open quantum system approach ¹ in the relativistic framework to a more general and practical scenario where not only are both the QB’s transverse and longitudinal spin components coupled to the quantum field, but also is the external driving considered to act on the system. We derive the analytical expression of the average energy stored in the QB and analyze how its dynamics is affected by the driving amplitude, BTZ spacetime properties, the boundary conditions on quantum field, and different dissipative couplings. We also investigate the corresponding charging stability in these scenarios after switching off the charging. Interestingly, it is found that which kind of dissipative coupling, decoherence or pure dephasing, leads to a better charging performance depends on the weight between the driving amplitude and the energy-level spacing of the QB. Besides, Hawking radiation may assist on the charging protocol under certain conditions, manifesting the improvement of the maximum average energy stored in the QB compared with the closed one. It means that one can extract energy from vacuum fluctuations in curved spacetime via dissipation in charging protocol.

Note that the BTZ spacetime is an exact solution of the Einstein equation in $(2 + 1)$ -

¹Usually, the system is assumed to be coupled to quantum field only with transverse component and without external driving.

dimensional gravity that is found by Máximo Bañados, Claudio Teitelboim, and Jorge Zanelli (BTZ) [71]. As a result of that, the BTZ solution might provide a concrete paradigm for general relativity in $(2 + 1)$ dimensions to explore the foundations of classical and quantum gravity [72, 73], and thus has attracted a lot attention. It has been found that the BTZ black hole has an event horizon and (in the rotating case) an inner horizon, appears as the final state of collapsing matter, and shares the thermodynamic properties much like those of $(3 + 1)$ -dimensional black hole. However, it is asymptotically anti-de Sitter rather than asymptotically flat, and has no curvature singularity at the origin, which are quite different from the Schwarzschild and Kerr solutions [74, 75]. Furthermore, in the BTZ spacetime, the Wightman functions for a conformally coupled scalar field (in the Hartle-Hawking vacuum) are known analytically [74, 76]. Until now, many interesting quantum phenomena associated with the BTZ spacetime has been explored, e.g., the response of the Unruh-DeWitt particle detectors [77], quantum fluctuations [78], correlation harvesting [79, 80], anti-Hawking effect [81–83], quantum signatures of black hole mass superpositions [63], Fisher information [56], Lamb shift [84], holographic complexity [85] and so on. As a further step, we are going to investigate, in the present paper, the dissipative dynamics of an open QB coupled with the fluctuating conformal massless scalar field in vacuum in the BTZ spacetime, hoping to further understand the properties of the BTZ spacetime in terms of charging protocol, as well as the dissipative dynamics of open QB in the relativistic framework.

The outline of this paper is as follows. In section 2 we present the model of a single cell QB coupled to a vacuum fluctuations of quantum field. The charging performance indicators, such as the average energy stored in the QB, are calculated here. In section 3 we consider the dynamics of the average energy stored when the open QB is located in the BTZ spacetime, and explore how the driving amplitude, BTZ spacetime properties, the boundary conditions on quantum field, and different dissipative couplings affect the charging performance, including both the dynamics of the average energy stored and the charging stability. Finally, discussions and summary of the main results are present in section 4.

2 The model

In this section we will introduce our open quantum battery model and the relevant physical quantities to characterize the charging and discharging performances of a quantum battery. In our paper, $\hbar = 1$ is set, σ_k ($k = x, y, z$) indicates the usual k -th Pauli matrix.

2.1 Open quantum battery model

A single cell QB is modeled as a two-level system with the following Hamiltonian,

$$H_{\text{QB}} = \frac{\Delta}{2} \sigma_z, \quad (2.1)$$

where Δ denotes the energy-level spacing between the system's ground and excited state, i.e., $|g\rangle$ and $|e\rangle$, which can be seen as the empty and the full cell configuration, respectively.

Note that we will consider all the physics in the framework of the QB which has the proper time τ . In order to explore the charging protocol, at time $\tau = 0^+$ we switch on the charger which is described by an external classical field A coupled with the σ_x component of the QB [9, 10, 17, 18],

$$H_C = -\frac{A}{2}\sigma_x. \quad (2.2)$$

In addition to that, the QB is assumed to be locally coupled to a fluctuating massless scalar field $\phi(x(\tau))$ in vacuum, which may result in dissipation of the QB. The field's Hamiltonian reads

$$H_F(\tau) = \int d^3k \omega_{\mathbf{k}} a_{\mathbf{k}}^\dagger a_{\mathbf{k}} \frac{dt}{d\tau}, \quad (2.3)$$

where $a_{\mathbf{k}}^\dagger$, $a_{\mathbf{k}}$ are the creation and annihilation operators of the scalar field. The specific QB-field coupling is assumed to be linear along both the longitudinal (z) and transverse (x) directions,

$$H_I = \mu(\sin \theta \sigma_z + \cos \theta \sigma_x) \phi(x(\tau)), \quad (2.4)$$

where μ is a small coupling constant. This interaction captures both decoherence ($\theta = 0$) and pure dephasing ($\theta = \pi/2$) processes.

To study the dynamical evolution of the QB, we start by considering an unitary rotation in the spin space $R(\Theta) = e^{-i\frac{\Theta}{2}\sigma_y}$, with the angle Θ chosen in such a way to project the QB-Charger part $H_{\text{QB}} + H_C$ only along the z axis. After this rotation, we can find

$$\begin{aligned} \tilde{H}_{\text{BQ}} &= RH_{\text{QB}}R^\dagger = \frac{\Delta}{2}(\cos \Theta \sigma_z + \sin \Theta \sigma_x), \\ \tilde{H}_C &= RH_C R^\dagger = \frac{A}{2}(\sin \Theta \sigma_z - \cos \Theta \sigma_x), \\ \tilde{H}_I &= RH_I R^\dagger = \mu(\sin(\theta - \Theta) \sigma_z + \cos(\theta - \Theta) \sigma_x) \phi(x(\tau)). \end{aligned} \quad (2.5)$$

Choosing $\cos \Theta = \Delta/\sqrt{\Delta^2 + A^2}$ and $\sin \Theta = A/\sqrt{\Delta^2 + A^2}$, then $\tilde{H}_{\text{BQ}} + \tilde{H}_C = \frac{1}{2}\sqrt{\Delta^2 + A^2}\sigma_z$. In the beginning, we assume the total state of the QB and the quantum field is prepared at $\rho_{\text{QB}}(0) \otimes |0\rangle\langle 0|$, where $\rho_{\text{QB}}(0) = \frac{1}{2}(\mathbf{I} + \vec{\mathbf{w}}(0) \cdot \vec{\sigma})$ is initial reduced density matrix of the QB, and $|0\rangle$ is the vacuum of the scalar field, defined by $a_{\mathbf{k}}|0\rangle = 0$ for all \mathbf{k} . Therefore, the rotated reduced initial matrix of the QB is $\tilde{\rho}_{\text{QB}}(0) = R(\Theta)\rho_{\text{QB}}(0)R^\dagger(\Theta) = \frac{1}{2}(\mathbf{I} + \vec{\mathbf{r}}(0) \cdot \vec{\sigma})$, satisfying

$$\begin{aligned} r_1(0) &= w_1(0) \cos \Theta + w_3(0) \sin \Theta, \\ r_2(0) &= w_2(0), \\ r_3(0) &= w_3(0) \cos \Theta - w_1(0) \sin \Theta. \end{aligned} \quad (2.6)$$

For the whole system, its equation of motion in the interaction picture yields

$$\frac{\partial \tilde{\rho}_{\text{tot}}(\tau)}{\partial \tau} = -i[\tilde{H}_I(\tau), \tilde{\rho}_{\text{tot}}(\tau)]. \quad (2.7)$$

Since we are interested in the dynamics of the QB, we trace over the degree of freedom of the field. Besides, in the limit of weak coupling between the QB and the field we perform the Born approximation and the Markov approximation [41]. From Eq. (2.7) we can finally find the evolution of the reduced density matrix $\tilde{\rho}_{\text{QB}}(\tau)$ can be written in the Lindblad master equation form [41, 42],

$$\frac{\partial \tilde{\rho}_{\text{QB}}(\tau)}{\partial \tau} = -i[\tilde{H}_{\text{eff}}, \tilde{\rho}_{\text{QB}}(\tau)] + \mathcal{L}[\tilde{\rho}_{\text{QB}}(\tau)], \quad (2.8)$$

where

$$\mathcal{L}[\tilde{\rho}] = \sum_{i=\pm, z} [L_i \tilde{\rho} L_i^\dagger - \frac{1}{2}(L_i^\dagger L_i \tilde{\rho} + \tilde{\rho} L_i^\dagger L_i)], \quad (2.9)$$

$$\tilde{H}_{\text{eff}} = \frac{1}{2}\Omega\sigma_z = \frac{1}{2}\{\sqrt{\Delta^2 + A^2} + \text{Im}(\Gamma_+ + \Gamma_-)\}\sigma_z. \quad (2.10)$$

Note \tilde{H}_{eff} is the effective Hamiltonian in which Ω denotes the effective energy level-spacing of the QB with correction term $\text{Im}(\Gamma_+ + \Gamma_-)$ being the Lamb shift. Usually the Lamb shift can be neglected because it is far less than $\sqrt{\Delta^2 + A^2}$, i.e., $\Omega \approx \sqrt{\Delta^2 + A^2}$. Besides, $L_+ = \sqrt{\gamma_+}\sigma_+$, $L_- = \sqrt{\gamma_-}\sigma_-$, $L_z = \sqrt{\gamma_z}\sigma_z$ with $\sigma_\pm = \frac{1}{2}(\sigma_x \pm i\sigma_y)$ and

$$\begin{aligned} \gamma_\pm &= 2\text{Re}\Gamma_\pm = \mu^2 \cos^2(\theta - \Theta) \int_{-\infty}^{+\infty} d\Delta\tau e^{\mp i\Omega\Delta\tau} G(x(\tau), x(\tau')), \\ \gamma_z &= \mu^2 \sin^2(\theta - \Theta) \int_{-\infty}^{+\infty} d\Delta\tau G(x(\tau), x(\tau')), \end{aligned} \quad (2.11)$$

where $G(x(\tau), x(\tau'))$ is the field Wightman function and $\Delta\tau = \tau - \tau'$.

We assume the time evolution density matrix of the QB can be written as

$$\tilde{\rho}_{\text{QB}}(\tau) = \frac{1}{2}(\mathbf{I} + \tilde{\mathbf{r}}(\tau) \cdot \vec{\sigma}), \quad (2.12)$$

so the corresponding initial state is $\tilde{\rho}_{\text{QB}}(0) = \frac{1}{2}(\mathbf{I} + \tilde{\mathbf{r}}(0) \cdot \vec{\sigma})$. Substituting the density matrix $\tilde{\rho}_{\text{QB}}(\tau)$ (2.12) into the master equation (2.8), the time dependent state parameters $\tilde{\mathbf{r}}(\tau)$ after a series of calculations are found to be

$$\begin{aligned} r_1(\tau) &= r_1(0) \cos(\Omega\tau) e^{-\frac{1}{2}(\gamma_+ + \gamma_- + 4\gamma_z)\tau} - r_2(0) \sin(\Omega\tau) e^{-\frac{1}{2}(\gamma_+ + \gamma_- + 4\gamma_z)\tau}, \\ r_2(\tau) &= r_1(0) \sin(\Omega\tau) e^{-\frac{1}{2}(\gamma_+ + \gamma_- + 4\gamma_z)\tau} + r_2(0) \cos(\Omega\tau) e^{-\frac{1}{2}(\gamma_+ + \gamma_- + 4\gamma_z)\tau}, \\ r_3(\tau) &= r_3(0) e^{-(\gamma_+ + \gamma_-)\tau} + \frac{\gamma_+ - \gamma_-}{\gamma_+ + \gamma_-} (1 - e^{-(\gamma_+ + \gamma_-)\tau}). \end{aligned} \quad (2.13)$$

Rotating $\tilde{\rho}_{\text{QB}}(\tau)$ in Eq. (2.12) with state parameters (2.13), we can obtain the evolving

state of the QB, $\rho_{\text{QB}}(\tau) = R^\dagger(\Theta)\tilde{\rho}_{\text{QB}}(\tau)R(\Theta)$.

2.2 Charging performance indicators

To characterize the charging performance, we first need to clarify the time evolution of the spin components $\langle\sigma_k(\tau)\rangle$ ($k = x, y, z$), which can be written as averages over the time dependent total density matrix, $\rho_{\text{tot}}(\tau)$ driven by the total Hamiltonian $H = H_{\text{QB}} + H_{\text{C}} + H_{\text{F}} + H_{\text{I}}$

$$\langle\sigma_k(\tau)\rangle = \text{Tr}[\rho_{\text{tot}}(\tau)\sigma_k]. \quad (2.14)$$

These averages can be represented in terms of the time dependent reduced density matrix $\rho(\tau)$ as

$$\langle\sigma_k(\tau)\rangle = \text{Tr}[\rho(\tau)\sigma_k], \quad (2.15)$$

where $\rho(\tau) = \text{Tr}_{\text{F}}[\rho_{\text{tot}}(\tau)]$, meaning that the degree of freedom of the field has been traced over.

Energy exchanges between the different subparts, and thus charging dynamics, at time τ can be then determined by studying the energy variations

$$\langle E_{\text{s}}(\tau)\rangle = \langle H_{\text{s}}(\tau)\rangle - \langle H_{\text{s}}(0)\rangle, \quad (2.16)$$

where $\text{s} = \text{QB}, \text{C}, \text{FI}$. Note that FI denotes the field plus the interaction between the field and the QB. Recall that for $\tau > 0$, since we have assumed that the driving is static, we have $\dot{H} = 0$, with an energy balance of the form

$$\langle E_{\text{QB}}(\tau)\rangle + \langle E_{\text{C}}(\tau)\rangle + \langle E_{\text{FI}}(\tau)\rangle = 0. \quad (2.17)$$

Note that this condition must hold for any driving amplitude and dissipation.

From now on, we calculate the average energy of the QB, $\langle H_{\text{QB}}(\tau)\rangle$, and that of the charger, $\langle H_{\text{C}}(\tau)\rangle$. Using the rotation $R(\Theta)$ and the expressions (2.5), we can directly obtain

$$\begin{aligned} \langle H_{\text{QB}}(\tau)\rangle &= \text{Tr}[H_{\text{QB}}\rho_{\text{QB}}(\tau)] = \text{Tr}[R(\Theta)H_{\text{QB}}R^\dagger(\Theta)R(\Theta)\rho_{\text{QB}}(\tau)R^\dagger(\Theta)] \\ &= \text{Tr}[\tilde{H}_{\text{QB}}\tilde{\rho}_{\text{QB}}(\tau)] = \frac{\Delta}{2} \left[\langle\sigma_z(\tau)\rangle \cos \Theta + \langle\sigma_x(\tau)\rangle \sin \Theta \right], \end{aligned} \quad (2.18)$$

$$\begin{aligned} \langle H_{\text{C}}(\tau)\rangle &= \text{Tr}[H_{\text{C}}\rho_{\text{C}}(\tau)] = \text{Tr}[R(\Theta)H_{\text{C}}R^\dagger(\Theta)R(\Theta)\rho_{\text{C}}(\tau)R^\dagger(\Theta)] \\ &= \text{Tr}[\tilde{H}_{\text{C}}\tilde{\rho}_{\text{C}}(\tau)] = \frac{A}{2} \left[\langle\sigma_z(\tau)\rangle \sin \Theta - \langle\sigma_x(\tau)\rangle \cos \Theta \right]. \end{aligned} \quad (2.19)$$

We can further calculate the above average energies using the solutions shown in (2.13). It

is given by

$$\begin{aligned}\langle H_{\text{QB}}(\tau) \rangle &= \frac{\Delta}{2} \left[r_3(\tau) \cos \Theta + r_1(\tau) \sin \Theta \right], \\ \langle H_C(\tau) \rangle &= \frac{A}{2} \left[r_3(\tau) \sin \Theta - r_1(\tau) \cos \Theta \right].\end{aligned}\tag{2.20}$$

Note that $r_3(\tau)$ and $r_1(\tau)$ depend on the field correlation function shown in (2.11), thus on the spacetime properties due to the scattering off quantum field. Therefore, one can expect that the charging dynamics depends on the spacetime properties, and in turn one can also learn the spacetime properties from the charging physics.

3 Quantum battery in BTZ spacetime

In this section, we consider the QB which is coupled to conformal massless scalar fields in vacuum in the BTZ spacetime. The corresponding line element of the BTZ spacetime can be written in Schwarzschild-like coordinates [71, 74, 86] as

$$ds^2 = -\frac{r^2 - M\ell^2}{\ell^2} dt^2 + \frac{\ell^2}{r^2 - M\ell^2} dr^2 + r^2 d\phi^2.\tag{3.1}$$

We can see from the above metric that, unlike the Schwarzschild black hole case, the BTZ black hole is asymptotically anti-de Sitter with a negative cosmological constant, $\Lambda = -1/\ell^2$. Besides, it has a horizon at $r_h = \sqrt{M}\ell$ with M denoting the mass of the BTZ solution.

To obtain the charging dynamics of the QB in the BTZ spacetime, we first need to know the Wightman function of the conformal scalar field which may capture the character of the quantum field vacuum fluctuations and plays an important role in the dynamics of the QB through the QB-field interaction. In this paper, we assume that the scalar field is in the Hartle-Hawking vacuum in the BTZ spacetime. It is interesting to note that the BTZ spacetime can be obtained by a topological identification of AdS_3 spacetime. Therefore, using the method of images, the corresponding Wightman function in the BTZ spacetime for the conformal massless scalar field in the Hartle-Hawking vacuum can be obtained in terms of the corresponding Wightman function in AdS_3 spacetime ² [74],

$$G_{\text{BTZ}}^+(x, x') = \sum_{n=-\infty}^{+\infty} G_{\text{AdS}}^+(x, \Gamma^n x'),\tag{3.2}$$

where $G_{\text{AdS}}^+(x, x')$ is the Wightman function in AdS_3 spacetime and $\Gamma x'$ represents the action of the identification $\phi \mapsto \phi + 2\pi$ on point x' . Assuming that the field satisfies different boundary conditions at spatial infinity due to lack of global hyperbolicity of the

²Go beyond the standard quantization of quantum field, an alternative quantization in AdS/CFT has been introduced in Ref. [87].

BTZ spacetime, the Wightman function can be found analytically as follows [74]

$$G_{\text{BTZ}}^+(x, x') = \frac{1}{4\sqrt{2\pi}\ell} \sum_{n=-\infty}^{\infty} \left[\frac{1}{\sqrt{\sigma_n}} - \frac{\zeta}{\sqrt{\sigma_n + 2}} \right], \quad (3.3)$$

where

$$\sigma_n = \frac{rr'}{r_h^2} \cosh \left[\sqrt{M}(\Delta\phi - 2\pi n) \right] - 1 - \frac{\sqrt{(r^2 - r_h^2)(r'^2 - r_h^2)}}{r_h^2} \cosh \left[\frac{r_h}{\ell^2} \Delta t \right], \quad (3.4)$$

with $\Delta\phi = \phi - \phi'$, and $\Delta t = t - t'$. The parameter $\zeta \in \{1, 0, -1\}$ respectively specifies the Dirichlet ($\zeta = 1$), transparent ($\zeta = 0$), and Neumann ($\zeta = -1$) boundary conditions satisfied by the field at spatial infinity [88].

In the following discussions, we assume that the QB is spatially fixed at a constant r in the BTZ spacetime such that $\Delta\phi = 0$, $\Delta\tau = \tau - \tau' = \sqrt{-g_{00}}\Delta t$. In this case, inserting the BTZ Wightman function from (3.3) into the QB state parameter (2.11), we can find

$$\begin{aligned} \gamma_+ &= \frac{\mu^2 \cos^2(\theta - \Theta)}{2} \left(\frac{1}{e^{\Omega/T} + 1} \right) \sum_{n=-\infty}^{n=\infty} \left[P_{-\frac{1}{2} + i\frac{\Omega}{2\pi T}}(\cosh \alpha_n) - \zeta P_{-\frac{1}{2} + i\frac{\Omega}{2\pi T}}(\cosh \beta_n) \right], \\ \gamma_- &= \frac{\mu^2 \cos^2(\theta - \Theta)}{2} \left(\frac{1}{e^{-\Omega/T} + 1} \right) \sum_{n=-\infty}^{n=\infty} \left[P_{-\frac{1}{2} - i\frac{\Omega}{2\pi T}}(\cosh \alpha_n) - \zeta P_{-\frac{1}{2} - i\frac{\Omega}{2\pi T}}(\cosh \beta_n) \right], \\ \gamma_z &= \frac{\mu^2 \sin^2(\theta - \Theta)}{4} \sum_{n=-\infty}^{n=\infty} \left[P_{-\frac{1}{2}}(\cosh \alpha_n) - \zeta P_{-\frac{1}{2}}(\cosh \beta_n) \right], \end{aligned} \quad (3.5)$$

where $P_\nu(x)$ represents the associated Legendre function of the first kind [89], satisfying $P_{-\frac{1}{2} + i\lambda} = P_{-\frac{1}{2} - i\lambda}$, T is the local KMS temperature given by

$$T = \frac{r_h}{2\pi\ell\sqrt{r^2 - r_h^2}}, \quad (3.6)$$

and the auxiliary functions $\cosh \alpha_n$ and $\cosh \beta_n$ have been defined as

$$\cosh \alpha_n = \frac{r_h^2}{r^2 - r_h^2} \left[\frac{r^2}{r_h^2} \cosh(2\pi n\sqrt{M}) - 1 \right], \quad (3.7)$$

$$\cosh \beta_n = \frac{r_h^2}{r^2 - r_h^2} \left[\frac{r^2}{r_h^2} \cosh(2\pi n\sqrt{M}) + 1 \right]. \quad (3.8)$$

Let us note that the local temperature of the BTZ spacetime can be rewritten in the following form

$$T = \frac{\sqrt{a_{\text{BTZ}}^2 - \ell^{-2}}}{2\pi} \quad (3.9)$$

with $a_{\text{BTZ}} = r/(\ell\sqrt{r^2 - r_h^2})$ representing the acceleration of the constant r trajectory in the BTZ spacetime. Here T is analogous to the temperature felt by an accelerated observer in AdS₃ spacetime [90]. It is demonstrated in Ref. [90] that there exists a critical acceleration, $1/\ell$, in AdS₃ spacetime, and only the observer with a constant super-critical acceleration a (i.e., $a > 1/\ell$) can register the quasi-thermal response with a temperature equal to $\sqrt{a^2 - \ell^{-2}}/(2\pi)$. Besides, from the response functions γ_{\pm} in (3.5) we can see that the Fermi-Dirac type distribution is displayed as noted in Ref. [74].

3.1 Charging dynamics

In this section we will study the charging performances in the presence of dissipation which results from the vacuum fluctuations in the BTZ spacetime.

We now use the previous results in order to describe the dynamics of the QB by setting different initial parameters. We will determine the energy variation associated to the charging process by considering the QB is initially prepared in the ground state $|g\rangle$, i.e., $w_1(0) = 0, w_2(0) = 0, w_3(0) = -1$ in $\rho_{\text{QB}}(0)$. Unless otherwise stated, we will discuss the two limiting case of decoherence coupling ($\theta = 0$ in Eq. (2.4)) and of pure dephasing coupling ($\theta = \pi/2$ in Eq. (2.4)).

Before discussing the dissipative dynamics, let us recall the scenario where the dissipation is absent, which corresponds to $\mu = 0$ case in the interaction Hamiltonian (2.4). In this case, all energy supplied by H_C is transferred to the QB, whose maximum energy that can be stored is given by the energy level spacing Δ . The QB then is charged by a static driving protocol according to [10, 91]

$$\langle E_{\text{QB}}(\tau) \rangle = \frac{\Delta A^2}{2 \Omega^2} [1 - \cos(\Omega\tau)], \quad (3.10)$$

where $\Omega = \sqrt{\Delta^2 + A^2}$ is the Rabi frequency. From (3.10) we can see that since the evolution of the closed QB is unitary, the charging and discharge processes of the QB behaves periodically. It is completely discharged (again empty and in the $|g\rangle$ state) when $\Omega\tau = 2\pi n$ ($n > 0$ integer). Note that the optimal charging time, when the energy stored reaches its maxima, is $\Omega\tau = \pi n$ ($n > 0$ odd numbers). In this case, the energy stored in the QB is

$$\langle E_{\text{QB}}(\tau) \rangle_{\text{max}} = \Delta \frac{A^2}{\Omega^2}. \quad (3.11)$$

This amount approaches its maxima for very large amplitude $A \gg \Delta$.

In the presence of dissipation, we first consider the case of decoherence coupling ($\theta = 0$ in Eq. (2.4)), where the QB-quantum field coupling only has the σ_x component. We find the corresponding average energy associated to the QB is given by

$$\langle E_{\text{QB}}(\tau) \rangle = \frac{\Delta}{2} \left\{ 1 - \frac{\Delta^2}{\Omega^2} e^{-\Gamma_0^r \tau} - \frac{\Delta}{\Omega} \left(\frac{e^{\Omega/T} - 1}{e^{\Omega/T} + 1} \right) (1 - e^{-\Gamma_0^r \tau}) - \frac{A^2}{\Omega^2} \cos(\Omega\tau) e^{-\Gamma_0 \tau} \right\}, \quad (3.12)$$

where

$$\begin{aligned}\Gamma_0^r &= \frac{\mu^2 \Delta^2}{2\Omega^2} \sum_{n=-\infty}^{n=\infty} \left[P_{-\frac{1}{2}+i\frac{\Omega}{2\pi T}}(\cosh \alpha_n) - \zeta P_{-\frac{1}{2}+i\frac{\Omega}{2\pi T}}(\cosh \beta_n) \right], \\ \Gamma_0 &= \frac{1}{2}\Gamma_0^r + \frac{\mu^2 A^2}{2\Omega^2} \sum_{n=-\infty}^{n=\infty} \left[P_{-\frac{1}{2}}(\cosh \alpha_n) - \zeta P_{-\frac{1}{2}}(\cosh \beta_n) \right].\end{aligned}\quad (3.13)$$

Similarly, the energy variation of the charger $\langle E_C(\tau) \rangle$ reads

$$\langle E_C(\tau) \rangle = \frac{A^2}{2\Omega} \left\{ -\frac{\Delta}{\Omega} e^{-\Gamma_0^r \tau} - \left(\frac{e^{\Omega/T} - 1}{e^{\Omega/T} + 1} \right) (1 - e^{-\Gamma_0^r \tau}) + \frac{\Delta}{\Omega} \cos(\Omega\tau) e^{-\Gamma_0 \tau} \right\}. \quad (3.14)$$

Note that dissipation effects are reflected in the incoherent relaxation rate, Γ_0^r , and dephasing rate, Γ_0 .

For the pure dephasing coupling case, it is described by setting $\theta = \pi/2$ in Eq. (2.4), where the QB-quantum field coupling only has the σ_z component. This coupling case may lead to a different dissipative dynamics compared with the decoherence case. Indeed, the corresponding average energy associated to the QB in this case can be found as

$$\langle E_{\text{QB}}(\tau) \rangle = \frac{\Delta}{2} \left\{ 1 - \frac{\Delta^2}{\Omega^2} e^{-\Gamma_{\pi/2}^r \tau} - \frac{\Delta}{\Omega} \left(\frac{e^{\Omega/T} - 1}{e^{\Omega/T} + 1} \right) (1 - e^{-\Gamma_{\pi/2}^r \tau}) - \frac{A^2}{\Omega^2} \cos(\Omega\tau) e^{-\Gamma_{\pi/2} \tau} \right\}, \quad (3.15)$$

and the charger contribution is given by

$$\langle E_C(\tau) \rangle = \frac{A^2}{2\Omega} \left\{ -\frac{\Delta}{\Omega} e^{-\Gamma_{\pi/2}^r \tau} - \left(\frac{e^{\Omega/T} - 1}{e^{\Omega/T} + 1} \right) (1 - e^{-\Gamma_{\pi/2}^r \tau}) + \frac{\Delta}{\Omega} \cos(\Omega\tau) e^{-\Gamma_{\pi/2} \tau} \right\} \quad (3.16)$$

where

$$\begin{aligned}\Gamma_{\pi/2}^r &= \frac{\mu^2 A^2}{2\Omega^2} \sum_{n=-\infty}^{n=\infty} \left[P_{-\frac{1}{2}+i\frac{\Omega}{2\pi T}}(\cosh \alpha_n) - \zeta P_{-\frac{1}{2}+i\frac{\Omega}{2\pi T}}(\cosh \beta_n) \right], \\ \Gamma_{\pi/2} &= \frac{1}{2}\Gamma_{\pi/2}^r + \frac{\mu^2 \Delta^2}{2\Omega^2} \sum_{n=-\infty}^{n=\infty} \left[P_{-\frac{1}{2}}(\cosh \alpha_n) - \zeta P_{-\frac{1}{2}}(\cosh \beta_n) \right].\end{aligned}\quad (3.17)$$

Let us turn our attention to analytically evaluating the average energy in some special cases. In the infinity time limit, i.e., $\tau \rightarrow \infty$, for both the decoherence and pure dephasing coupling cases the average energies in (3.12), (3.14), (3.15), (3.16) approaches to

$$\begin{aligned}\langle E_{\text{QB}}(\infty) \rangle &= \frac{\Delta}{2} \left\{ 1 - \frac{\Delta}{\Omega} \left(\frac{e^{\Omega/T} - 1}{e^{\Omega/T} + 1} \right) \right\}, \\ \langle E_C(\infty) \rangle &= -\frac{A^2}{2\Omega} \left(\frac{e^{\Omega/T} - 1}{e^{\Omega/T} + 1} \right).\end{aligned}\quad (3.18)$$

We note that in the infinity evolution time limit the average energies for the QB and charger

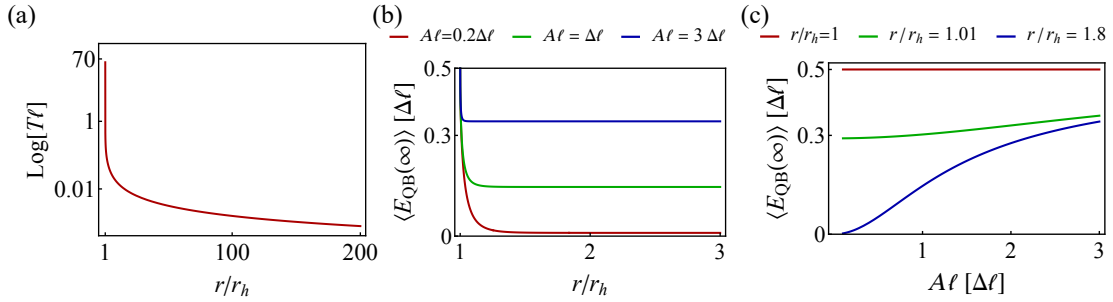


Figure 1. (a) The Hawking temperature shown in Eq. (3.9) as a function of the relative distance r/r_h of the QB; (b) The average energy stored in the QB $\langle E_{\text{QB}}(\infty) \rangle$ shown in Eq. (3.18) (in units $\Delta\ell$) as a function of the relative distance r/r_h ; (c) The average energy stored in the QB $\langle E_{\text{QB}}(\infty) \rangle$ shown in Eq. (3.18) (in units $\Delta\ell$) as a function of the charging amplitude $A\ell$.

are independent of the kinds of dissipation. Besides, in this case the average energies do not depend on the charging time, and is quite different from the case without dissipation shown in (3.10), which is always periodic with the charging time.

In Fig. 1 we show the Hawking temperature (3.9) and the average energy (3.18) stored in the QB in the infinity charging time. The temperature decreases monotonously as the increase of the distance of the QB away from the BTZ black hole horizon r/r_h . In the infinity charging time limit, the average energy stored in the QB approaches to $\lim_{r/r_h \rightarrow 1} \langle E_{\text{QB}}(\infty) \rangle = \frac{\Delta}{2}$ when the QB is located near the horizon, which does not depend on the charging amplitude A . This average energy decreases sharply with the increase of the relative distance r/r_h when near the horizon. While far away from the horizon it approaches to a constant $\lim_{r/r_h \rightarrow \infty} \langle E_{\text{QB}}(\infty) \rangle = \frac{\Delta}{2} \left(1 - \frac{\Delta}{\Omega}\right)$ which depends on the charging amplitude. We can find that when QB far away from the horizon the stronger the charging amplitude is, the more the average energy stored in the QB is. It means that, in the presence of dissipation, larger driving amplitude A leads to better charging of the QB. We can also see this behavior in Fig. 1 (c). Furthermore, the further the QB locates away from the black hole horizon, the more strongly its average energy in the infinite time limit depends on the charging amplitude A . This is because that when far away from the black hole horizon, the Hawking temperature in (3.9) approaches to vanishment, the dissipation of the QB effectively coming from the vacuum fluctuations of the quantum field could be considered to be weak. In this case the charger thus would play a dominated role in the whole charging process.

An interesting question is that in the presence of dissipation from vacuum field fluctuations in the BTZ spacetime, whether the maximum average energy stored in QB could be enhanced. We will compare $\langle E_{\text{QB}}(\infty) \rangle$ shown in (3.18) with $\langle E_{\text{QB}}(\tau) \rangle_{\text{max}}$ shown in (3.11), through defining

$$\delta E = \langle E_{\text{QB}}(\infty) \rangle - \langle E_{\text{QB}}(\tau) \rangle_{\text{max}} = \frac{\Delta}{2} \left[1 - \frac{\Delta}{\Omega} \left(\frac{e^{\Omega/T} - 1}{e^{\Omega/T} + 1} \right) - \frac{2A^2}{\Omega^2} \right]. \quad (3.19)$$

When $A \geq \Delta$, we can always find that the average-energy difference in this case is smaller

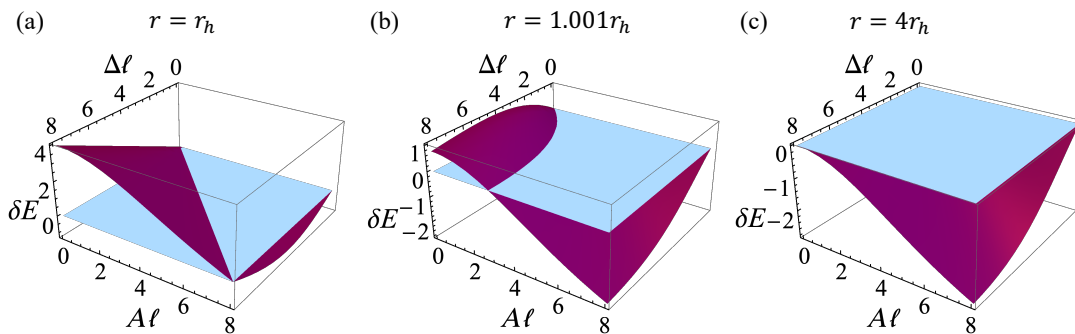


Figure 2. The average-energy difference stored in the QB between the dissipation case and the closed QB case shown in (3.19), as a function of the QB energy-level spacing $\Delta\ell$ and the charging amplitude $A\ell$. The location of the QB is: (a) $r = r_h$; (b) $r = 1.001r_h$; (c) $r = 4r_h$. The purple surface denotes the average-energy difference, while the bluish surface denotes $\delta E = 0$ surface.

than zero, $\delta E \leq 0$. Which means that the dissipation from vacuum field fluctuations in the BTZ spacetime might causes a worse charging performance compared with the closed QB case. Besides, if $T \gg \Omega$, we can find in Eq. (3.19) $\delta E \simeq \frac{\Delta}{2}(1 - 2A^2/\Omega^2) = \Delta(\Delta^2 - A^2)/2\Omega^2$. While for $T \ll \Omega$, we can find $\delta E \simeq \frac{\Delta}{2}(1 - \Delta/\Omega - 2A^2/\Omega^2)$. In these two cases, whether the charging performance in the presence of dissipation is better or worse than the closed QB charging case depends on the QB energy-level spacing Δ and the charging amplitude A . In Fig. 2 we plot the average-energy difference shown in (3.19) as a function of the QB energy-level spacing $\Delta\ell$ and the charging amplitude $A\ell$. We can find that the location of the QB (or equivalently the Hawking temperature), r (or T), affects the charging performance very much. When the QB is relatively far away from the horizon r_h , the average energy stored in QB in the presence of dissipation would never be more than that for the closed QB case. Thus when the Hawking temperature is relatively smaller, the dissipation from vacuum field fluctuations in the BTZ spacetime causes harmful influence on the charging performance. However, we can also find that when the QB approaches to the horizon, where the Hawking temperature is higher, the average energy shored in the QB in the presence of dissipation might be more than that for the closed QB case under the condition, $T \geq \Omega / \ln \left[\frac{\Delta\Omega + \Delta^2 - A^2}{\Delta\Omega + A^2 - \Delta^2} \right]$ with $\Delta > A$. It means in this case the dissipation from vacuum field fluctuations in the BTZ spacetime might enhance the charging performance. In other words, one can extract the energy from the vacuum fluctuations in curved space through dissipation in the charging process.

3.2 Effect of dissipation on average energy

We now discuss the results obtained above, showing how the effects of dissipation from vacuum field fluctuations in the BTZ spacetime modify the charging dynamics of the QB.

3.2.1 $\Delta < A$ case

In Fig. 3 we show the time evolution of the average energy stored in the QB $\langle E_{\text{QB}}(\tau) \rangle$ shown in Eq. (3.12) for the decoherence coupling case ($\theta = 0$ case). We fixed the energy-level spacing of the QB $\Delta\ell = 0.1$, the charging amplitude $A\ell = 0.2$, and the BTZ black

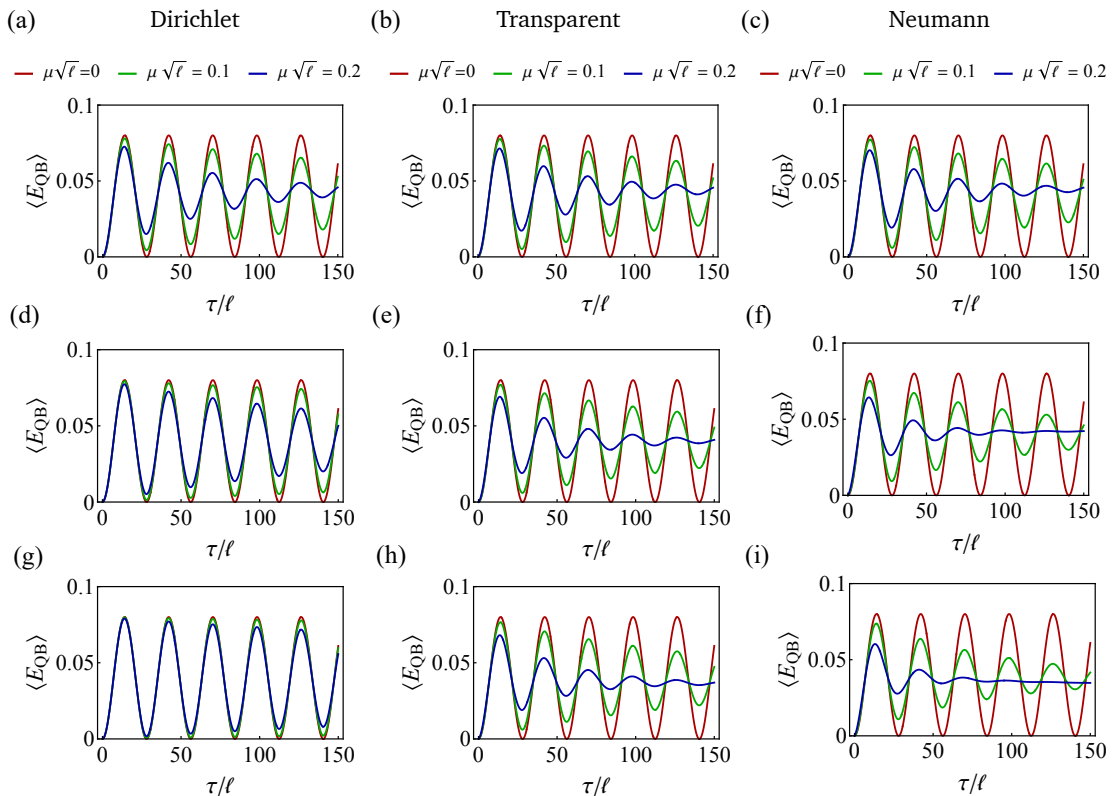


Figure 3. Time evolution of the average energy stored in the QB $\langle E_{\text{QB}}(\tau) \rangle$ shown in Eq. (3.12) for the decoherence coupling case with $\theta = 0$. Three different boundary conditions in BTZ spacetime are shown for various coupling strength $\mu\sqrt{\ell}$. Here we have taken the energy-level spacing $\Delta\ell = 0.1$, the charging amplitude $A\ell = 0.2$, and the mass $M = 1$. The first, second, and third row panels have taken the relative distance of the QB in BTZ spacetime $r/r_h = 1.001$, $r/r_h = 1.2$ and $r/r_h = 1.8$, respectively.

hole mass $M = 1$. Representative examples of different distance of the QB (or Hawking temperature) away from the horizon $r/r_h = 1.001$ (Fig. 3 (a), (b) and (c)), $r/r_h = 1.2$ (Fig. 3 (d), (e) and (f)), and $r/r_h = 1.8$ (Fig. 3 (g), (h) and (i)) have been chosen. The closed QB system driven by a static bias (see Eq. (3.10)) is also reported as a reference limit (see red curves). It is found that, in the presence of dissipation, the charged average energy presents a damped oscillatory behavior, whose amplitude is modulated by the exponential decay dictated by the incoherent relaxation and dephasing rates given in Eqs. (3.13). With the increase of the Hawking temperature, the damping strength is enhanced, and the average energy stored in the QB degrades faster to its asymptotic limit (3.18) for the Dirichlet boundary case, while it is opposite for the transparent and the Neumann boundary cases. The coupling strength $\mu\sqrt{\ell}$ could also enhance the dissipation as expected, showing stronger damping with the increase of the coupling strength. Besides, boundary conditions play an important role in the charging process. Although the boundary conditions do not change the average energy in the infinite charging time limit shown in (3.18), they could lead to different damping. We can see that the Neumann boundary

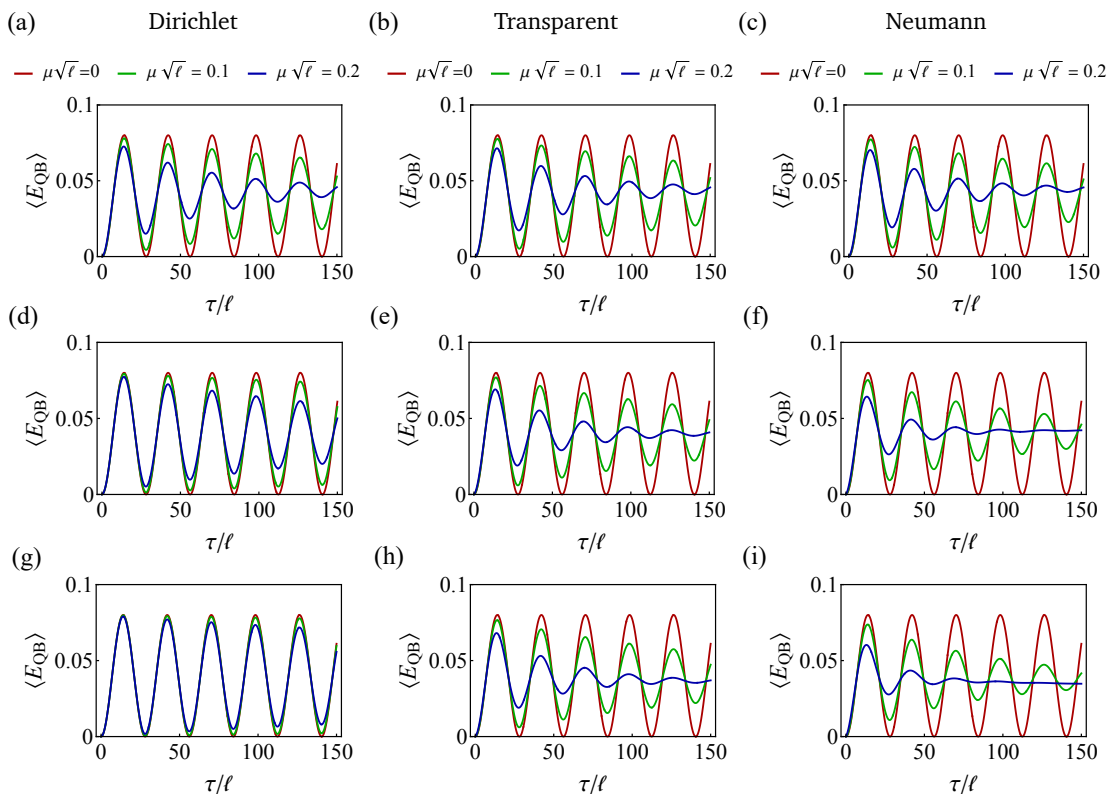


Figure 4. Time evolution of the average energy stored in the QB $\langle E_{\text{QB}}(\tau) \rangle$ shown in Eq. (3.15) for the pure dephasing coupling case with $\theta = \pi/2$. Three different boundary conditions in BTZ spacetime are shown for various coupling strength $\mu\sqrt{\ell}$. Here we have taken the energy level spacing $\Delta\ell = 0.1$, the charging amplitude $A\ell = 0.2$, and the mass $M = 1$. The first, second, and third row panels have taken the relative distance of the QB in BTZ spacetime $r/r_h = 1.001$, $r/r_h = 1.2$ and $r/r_h = 1.8$, respectively.

condition causes stronger damping than the transparent one, while the transparent one induces stronger damping than the Dirichlet one. This difference is more clear when the Hawking temperature becomes smaller.

In Fig. 4 we show the time evolution of the average energy stored in the QB $\langle E_{\text{QB}}(\tau) \rangle$ shown in Eq. (3.15) for the pure dephasing coupling case with $\theta = \pi/2$. As comparison, we fixed the same energy-level spacing of the QB $\Delta\ell = 0.1$, the charging amplitude $A\ell = 0.2$, and the BTZ black hole mass $M = 1$ as that in Fig. 3. We find that in the presence of dissipation all curves present a damped oscillatory behaviour, whose amplitude is modulated by the exponential decay dictated by the incoherent relaxation and dephasing rates given in Eqs. (3.17). These rate expressions are different from that for the decoherence coupling case discussed above, and thus may give rise to different relaxation dynamics as shown in the figure. It is evident that the average energy stored in the QB $\langle E_{\text{QB}}(\tau) \rangle$ shown in Eq. (3.12), when varying boundary conditions, coupling strength, and the relative distance of the QB, shares the same behaviour as that for the decoherence coupling case discussed above. However, they are different quantitatively.

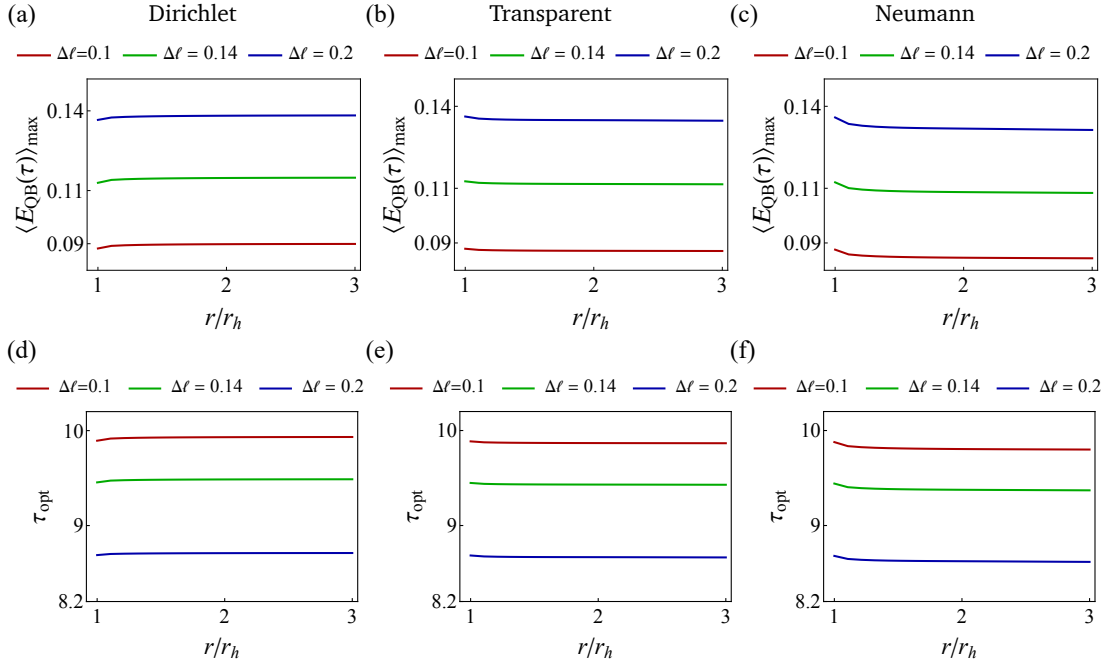


Figure 5. The maximum average energy stored in the QB $\langle E_{\text{QB}}(\tau) \rangle_{\text{max}}$, (a), (b), (c), and the optimal charging time τ_{opt} , (d), (e), (f), as a function of the relative distance of the QB in BTZ spacetime r/r_h for the decoherence coupling case ($\theta = 0$). Three different boundary conditions in BTZ spacetime are shown for various energy-level spacing $\Delta\ell$. Here we have taken the coupling strength $\mu\sqrt{\ell} = 0.1$, the charging amplitude $A\ell = 0.3$, and the mass $M = 1$.

For both the decoherence and the pure dephasing coupling cases, there is an optimal charging time, τ_{opt} , at which the average energy stored in the QB takes the maxima. In Figs. 5 and 6 we plot this maximum average energy and the optimal charging time as a function of the Hawking temperature parameter r/r_h by varying the energy-level spacing $\Delta\ell$ and the charging amplitude $A\ell$ for decoherence coupling case ($\theta = 0$). We can see from Fig. 5 that the boundary condition influences the behavior of the maximum average energy and the optimal charging time vs the Hawking temperature parameter significantly. For the Dirichlet case, the maximum average energy and the optimal charging time increase with the decrease of Hawking temperature (Hawking temperature decreases with the increase of r/r_h , see Fig. 1). When the Hawking temperature approaches to zero, these two quantities approach to asymptotical value. However, we can find that for both the transparent case and the Neumann case, the maximum average energy and the optimal charging time decrease when the Hawking temperature decreases. These two quantities, when the Hawking temperature goes to zero, also approach to asymptotical value. Besides, no matter for which boundary conditions, we can find that when the charging amplitude $A\ell$ and the Hawking temperature are fixed, the maximum average energy increases with the increase of the energy-level spacing of the QB $\Delta\ell$, while the corresponding optimal charging time decreases. In Fig. 6 we fix the energy-level spacing of the QB, $\Delta\ell$, and plot the maximum average energy stored in the QB $\langle E_{\text{QB}}(\tau) \rangle_{\text{max}}$ and

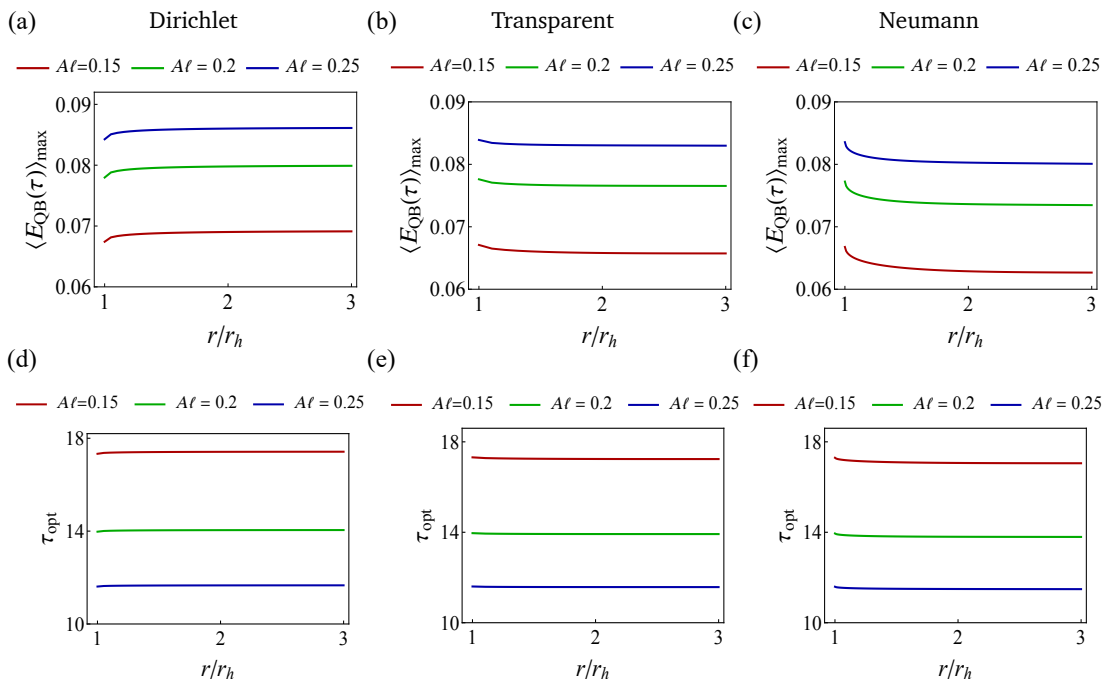


Figure 6. The maximum average energy stored in the QB $\langle E_{\text{QB}}(\tau) \rangle_{\text{max}}$, (a), (b), (c), and the optimal charging time τ_{opt} , (d), (e), (f), as a function of the relative distance of the QB in BTZ spacetime r/r_h for the decoherence coupling case ($\theta = 0$). Three different boundary conditions in BTZ spacetime are shown for various charging amplitude $A\ell$. Here we have taken the coupling strength $\mu\sqrt{\ell} = 0.1$, the energy-level spacing $\Delta\ell = 0.1$, and the mass $M = 1$.

the optimal charging time τ_{opt} as a function of the relative distance of the QB in BTZ spacetime r/r_h for various charging amplitude $A\ell$. We can also find that the boundary condition influences the behavior of the maximum average energy and the optimal charging time vs the Hawking temperature parameter significantly. When the relative distance of the QB in BTZ spacetime r/r_h approaches to the infinity, both the maximum average energy and the optimal charging time approach to asymptotical value. Furthermore, no matter for which boundary conditions, the maximum average energy increases with the increase of the charging amplitude, while the optimal charging time decreases when the energy-level spacing of the QB and the Hawking temperature are fixed.

In Figs. 7 and 8 we plot the maximum average energy and the optimal charging time as a function of the Hawking temperature parameter r/r_h by varying the energy-level spacing $\Delta\ell$ and the charging amplitude $A\ell$ for pure dephasing coupling case ($\theta = \pi/2$). We can find for this pure dephasing coupling case the maximum average energy and the optimal charging time share the same behaviors as that for the decoherence case shown in Figs. 5 and 6, while their magnitudes are different. This is because for both the decoherence case and the pure dephasing case their corresponding average energy associated to the QB share the same formula shown in (3.12) and (3.15), but with different incoherent relaxation and dephasing rates shown in (3.13) and (3.17).

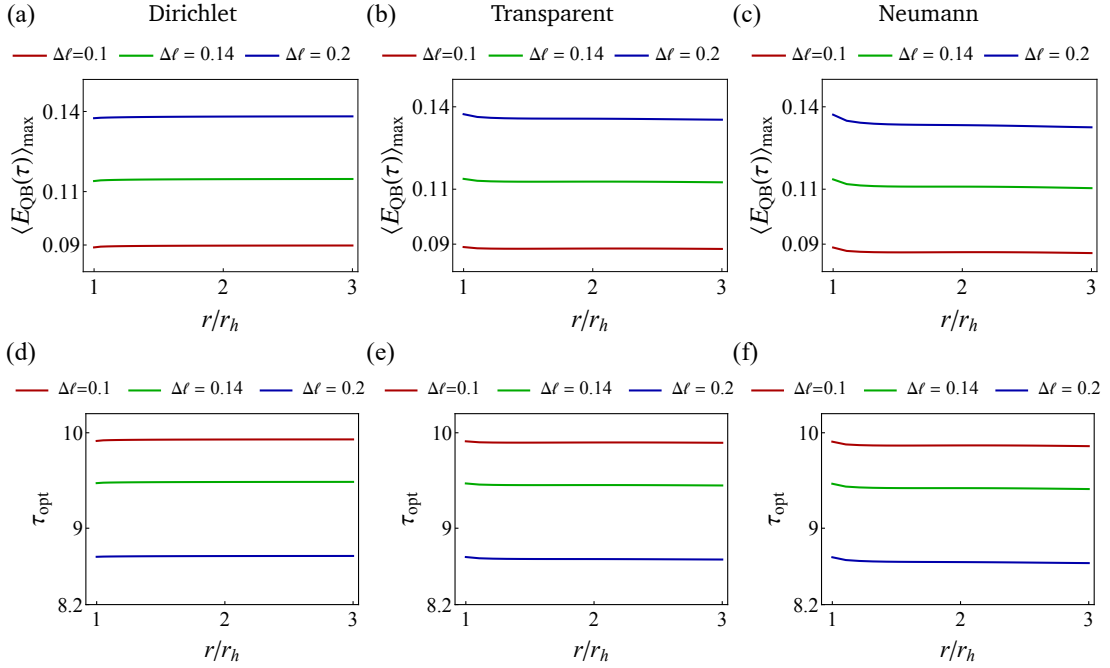


Figure 7. The maximum average energy stored in the QB $\langle E_{\text{QB}}(\tau) \rangle_{\text{max}}$, (a), (b), (c), and the optimal charging time τ_{opt} , (d), (e), (f), as a function of the relative distance of the QB in BTZ spacetime r/r_h for pure dephasing coupling case with $\theta = \pi/2$. Three different boundary conditions in BTZ spacetime are shown for various energy-level spacing $\Delta\ell$. Here we have taken the coupling strength $\mu\sqrt{\ell} = 0.1$, the charging amplitude $A\ell = 0.3$, and the mass $M = 1$.

3.2.2 $\Delta \geq A$ case

To consider the charging dynamics for $\Delta \geq A$ case, we in Fig. 9 plot the time evolution of the average energy stored in the QB $\langle E_{\text{QB}}(\tau) \rangle$ shown in Eq. (3.12) for the decoherence coupling case ($\theta = 0$). We fix the energy-level spacing of the QB $\Delta\ell = 0.13$, the charging amplitude $A\ell = 0.1$, and the mass $M = 1$. Representative examples of different distance of the QB (or Hawking temperature) away from the horizon $r/r_h = 1.001$ (Fig. 9 (a), (b) and (c)), $r/r_h = 1.1$ (Fig. 9 (d), (e) and (f)), and $r/r_h = 1.8$ (Fig. 9 (g), (h) and (i)) have been chosen. The closed QB system driven by a static bias (see Eq. (3.10)) is also reported as a reference limit (see red curves). It is found that, in the presence of dissipation, the charged average energy presents an oscillatory behavior in the early time, while it will finally approach a maximum for the long enough charging time if the Hawking temperature is high. This maximum average energy depends on the Hawking temperature, the charging amplitude $A\ell$, and the energy-level spacing of the QB $\Delta\ell$. Interestingly, unlike the $\Delta < A$ case, when $\Delta > A$ the maximum average energy might be more than that for the closed QB case if the Hawking temperature is high enough. Note that this advantage could occur for all the three different boundary condition cases, including the Dirichlet, the transparent, and the Neumann one. This means that the dissipation from vacuum field fluctuations in the BTZ spacetime might enhance the charging performance. In other words, through the interaction between the QB and the external quantum field

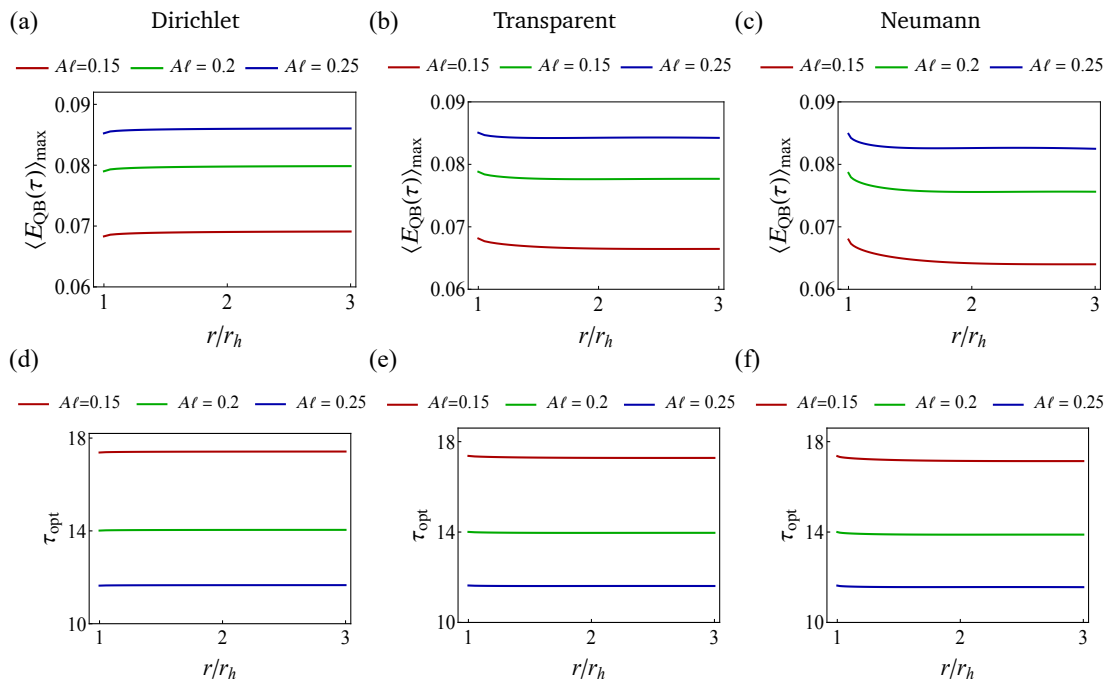


Figure 8. The maximum average energy stored in the QB $\langle E_{\text{QB}}(\tau) \rangle_{\text{max}}$, (a), (b), (c), and the optimal charging time τ_{opt} , (d), (e), (f), as a function of the relative distance of the QB in BTZ spacetime r/r_h for pure dephasing coupling case with $\theta = \pi/2$. Three different boundary conditions in BTZ spacetime are shown for various charging amplitude $A\ell$. Here we have taken the coupling strength $\mu\sqrt{\ell} = 0.1$, the energy-level spacing $\Delta\ell = 0.1$, and the mass $M = 1$.

one can in principle extract the energy from the vacuum fluctuations in curved space through dissipation in the charging process. Furthermore, we can also find that for the Dirichlet boundary case the average energy reaches a maximum earlier with the increase of the Hawking temperature. However, for the transparent boundary and the Neumann boundary cases when the Hawking temperature becomes higher, the average energy reaches the corresponding maximum later. Further comparing the average-energy dynamics for these three boundary condition cases, we can find that under the same conditions the average energy for the Neumann boundary case would be the first to reach a maximum value, then it is the transparent boundary case, and finally it is the Dirichlet one. We can also find that the stronger the coupling between the QB and the quantum field is, the earlier the QB reaches the maximum average energy during the charging process. However, the maximum value of the average energy does not depend on the coupling strength. This conclusion is valid for all the three boundary condition cases.

In Fig. 10 we plot the time evolution of the average energy stored in the QB $\langle E_{\text{QB}}(\tau) \rangle$ shown in Eq. (3.15) for the pure dephasing coupling case ($\theta = \pi/2$). We also fixed the energy-level spacing of the QB $\Delta\ell = 0.13$, the charging amplitude $A\ell = 0.1$, and the mass $M = 1$. Representative examples of different distance of the QB (or Hawking temperature) away from the horizon $r/r_h = 1.001$ (Fig. 10 (a), (b) and (c)), $r/r_h = 1.1$ (Fig. 10 (d), (e) and (f)), and $r/r_h = 1.8$ (Fig. 10 (g), (h) and (i)) have been chosen. We also choose

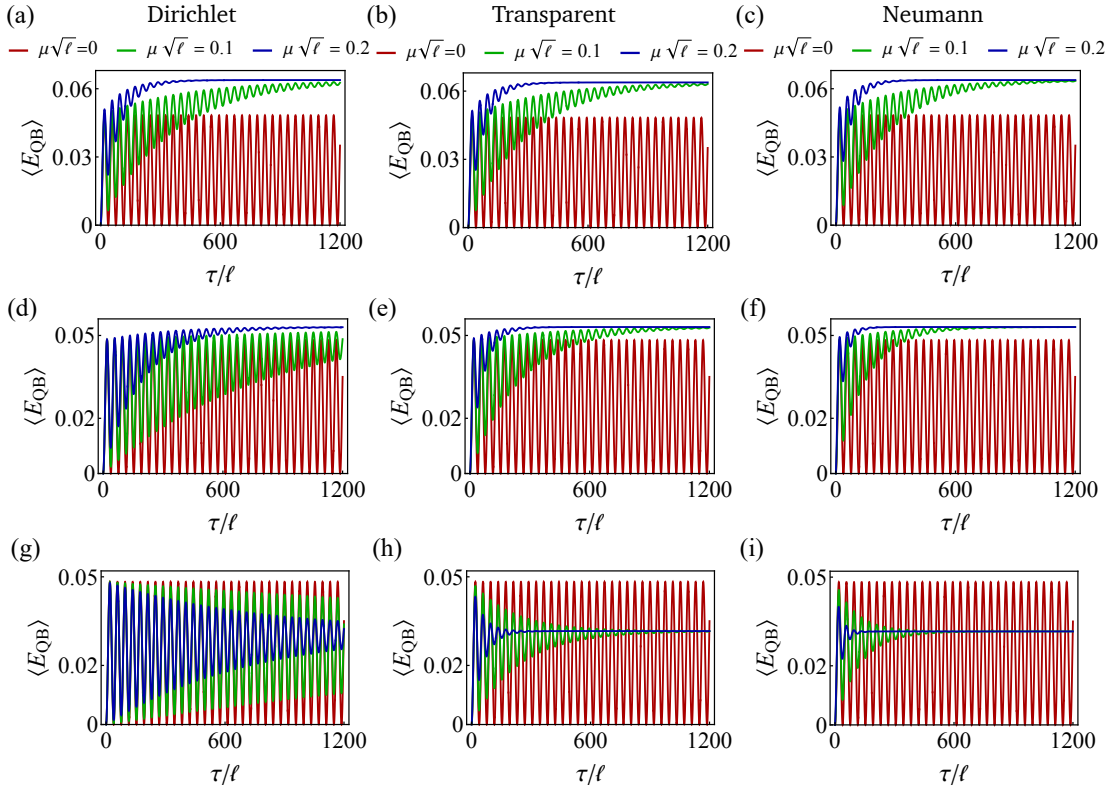


Figure 9. Time evolution of the average energy stored in the QB $\langle E_{\text{QB}}(\tau) \rangle$ shown in Eq. (3.12) for the decoherence coupling case ($\theta = 0$). Three different boundary condition cases in BTZ spacetime are shown for various coupling strength $\mu\sqrt{\ell}$. Here we have taken the energy level spacing $\Delta\ell = 0.13$, the charging amplitude $A\ell = 0.1$, and the mass $M = 1$. The first, second, and third row panels have taken the relative distance of the QB in BTZ spacetime $r/r_h = 1.001$, $r/r_h = 1.1$ and $r/r_h = 1.8$, respectively.

the closed QB system driven by a static bias (see Eq. (3.10)) as a reference limit (see red curves). Since the average energy for the dephasing coupling case has the similar formula to that for the decoherence coupling case, seen from Eqs. (3.12) and (3.15), we can find that the average energy for the dephasing coupling case shares the similar dynamics to that for the decoherence coupling case discussed above. Specifically, although in the presence of dissipation the charged average energy presents an oscillatory behavior in the early time, finally it will reach a constant if the charging time is long enough. This constant average energy denotes the maximum average energy of the QB during the charging process if the Hawking radiation is high enough, satisfying $T \geq \Omega / \ln \left[\frac{\Delta\Omega + \Delta^2 - A^2}{\Delta\Omega + A^2 - \Delta^2} \right]$ as discussed above. It is interesting that the maximum average energy for this case is stored more in the QB than that for the closed QB case. This result is quite different compared with $\Delta < A$ scenario where the maximum average energy in the presence of dissipation would never be more than that for the closed QB case. For all the three boundary condition cases, this maximum average energy increases with the increase of the Hawking temperature, while it does not depend on the coupling strength between the QB and the external quantum

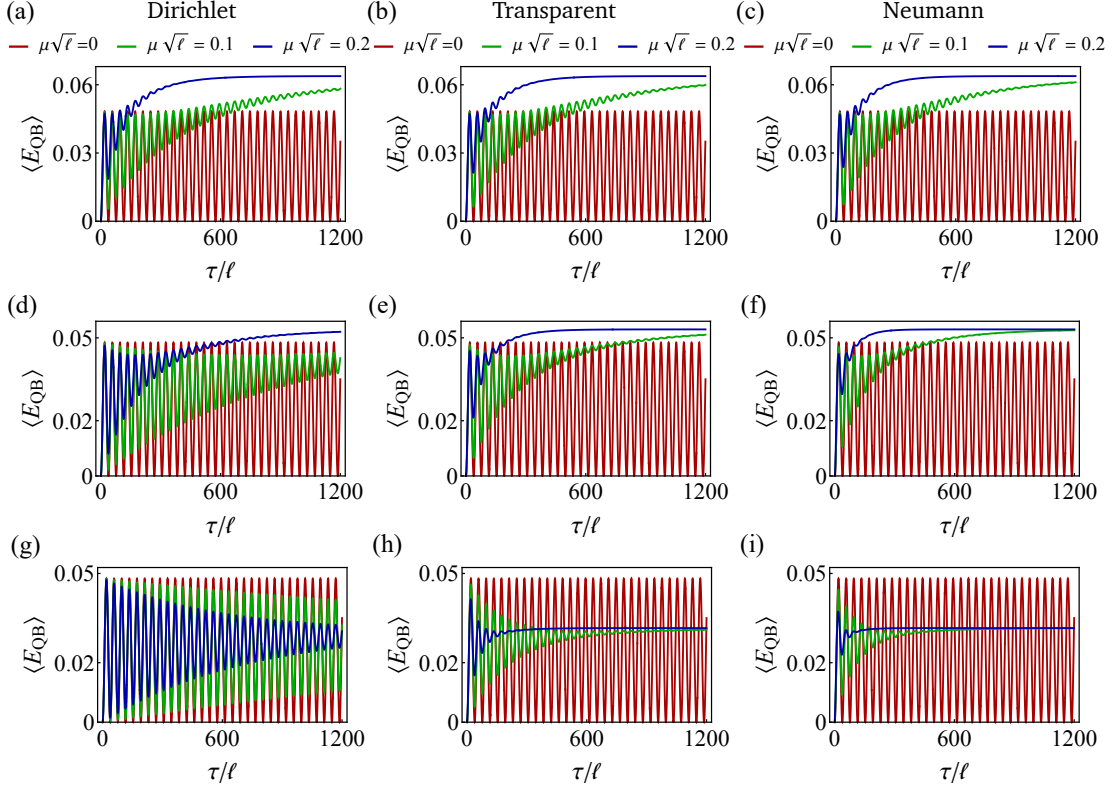


Figure 10. Time evolution of the average energy stored in the QB $\langle E_{\text{QB}}(\tau) \rangle$ shown in Eq. (3.12) for the pure dephasing coupling case ($\theta = \pi/2$). Three different boundary condition cases in BTZ spacetime are shown for various coupling strength $\mu\sqrt{\ell}$. Here we have taken the energy level spacing $\Delta\ell = 0.13$, the charging amplitude $A\ell = 0.1$, and the mass $M = 1$. The first, second, and third row panels have taken the relative distance of the QB in BTZ spacetime $r/r_h = 1.001$, $r/r_h = 1.1$ and $r/r_h = 1.8$, respectively.

field. However, the coupling strength would affect the time at which the average energy reaches the maximum. It is found that no matter for which boundary cases, the stronger the coupling is, the earlier the average energy reaches the maximum. Comparing the three different boundary cases, we can find for the Dirichlet boundary case the higher Hawking temperature may lead to the earlier maximum average energy that is reached by the QB, while this is quite the opposite for the other two boundary cases.

We give a brief summary here: we can find that the dynamics of the average energy stored in the QB during the charging process depends on the quantum field boundary condition, the coupling form between the QB and external quantum field, Hawking temperature, the QB energy-level spacing, and the charging amplitude. It is shown that under certain conditions the maximum average energy stored in an open QB might be more than that for the closed QB case. This advantage could occur for all the three different boundary condition cases, including the Dirichlet, the transparent, and the Neumann one. It means that the dissipation from vacuum field fluctuations in the BTZ spacetime might enhance the charging performance.

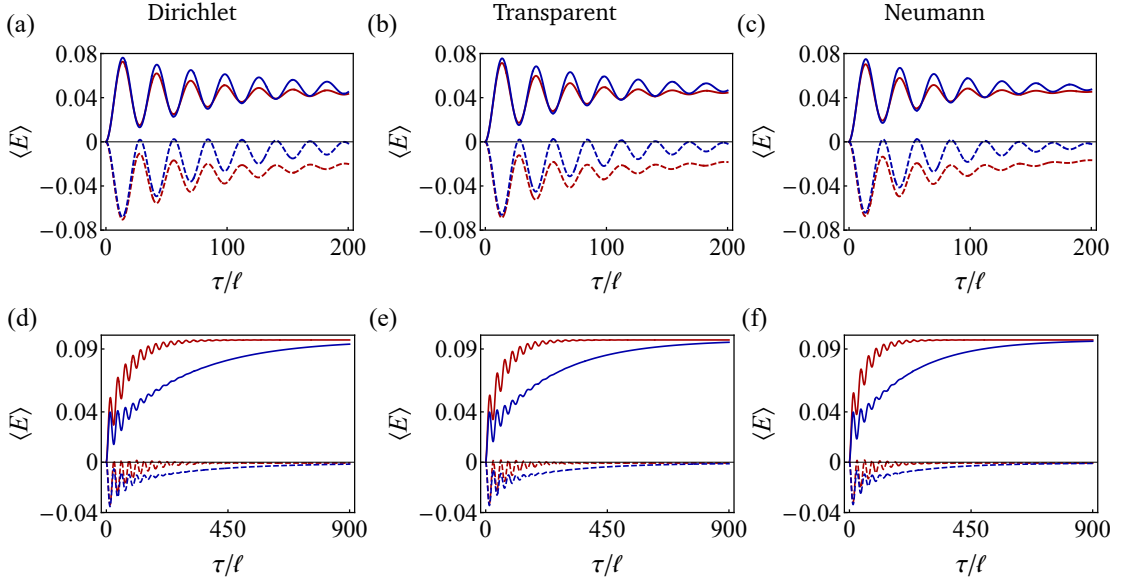


Figure 11. Time evolution of the average energy variation $\langle E \rangle$ for $Al = 0.2 > \Delta\ell = 0.1$ cases (a), (b), (c) and for $Al = 0.1 < \Delta\ell = 0.2$ cases (d), (e), (f). Solid red and blue lines associated to the QB correspond to the case of decoherence ($\theta = 0$) and pure dephasing ($\theta = \pi/2$) interaction with the quantum field, respectively; and dashed red and blue lines are associated to the charger. Here we have taken the mass $M = 1$, the relative distance of the QB in BTZ spacetime $r/r_h = 1.001$, the coupling strength $\mu\sqrt{\ell} = 0.2$, respectively.

3.3 Direct comparison of $\langle E \rangle$ for different coupling form

To better understand the charging performance in the presence of different dissipation, we directly compare two dissipative coupling schemes in Fig. 11. Two different driving amplitudes are considered, i.e., $Al = 0.2 > \Delta\ell = 0.1$ and $Al = 0.1 < \Delta\ell = 0.2$ with coupling strength $\mu\sqrt{\ell} = 0.2$. For $Al > \Delta\ell$ case the plots show that in the case $\theta = \pi/2$ (the pure dephasing coupling case) it is possible to achieve a better charging of QB (higher values of the maxima) compared with the decoherence coupling case ($\theta = 0$) in the finite time regime. This difference results from the different form of the dissipation rates in Eqs. (3.13), (3.17), where we can find the dephasing coupling case is less affected by dissipation. Indeed, since we consider $r/r_h \rightarrow 1$ (i.e., $T \rightarrow \infty$), Eqs. (3.12) and (3.15) reduce to

$$\langle E_{\text{QB}}(\tau) \rangle \approx \frac{\Delta}{2} \left\{ 1 - \frac{\Delta^2}{\Omega^2} e^{-\Gamma_0^r \tau} - \frac{A^2}{\Omega^2} \cos(\Omega\tau) e^{-\Gamma_0 \tau} \right\}, \quad (3.20)$$

and

$$\langle E_{\text{QB}}(\tau) \rangle \approx \frac{\Delta}{2} \left\{ 1 - \frac{\Delta^2}{\Omega^2} e^{-\Gamma_{\pi/2}^r \tau} - \frac{A^2}{\Omega^2} \cos(\Omega\tau) e^{-\Gamma_{\pi/2} \tau} \right\}, \quad (3.21)$$

respectively. We can numerically analyze the above conclusion from their corresponding rates, e.g, for chosen parameters of Fig. 11 (a), the corresponding rates are $\Gamma_0^r \simeq 0.00349\ell$, $\Gamma_0 = 0.0157\ell$ and $\Gamma_{\pi/2}^r \simeq 0.01396\ell$, $\Gamma_{\pi/2} = 0.01047\ell$, respectively. Since $\Gamma_0^r < \Gamma_{\pi/2}^r$, the

smaller relaxation rate (characterized by Γ_0^r and $\Gamma_{\pi/2}^r$) would lead to the smaller average energy with respect to the evolution time. Furthermore, the dephasing rate (characterized by Γ_0 and $\Gamma_{\pi/2}$) leads to the damping of oscillations (see in Figs. 11 (a), (b) and (c)). Because $\Gamma_0 > \Gamma_{\pi/2}$, the oscillatory amplitude of the average energy for the decoherence coupling case ($\theta = 0$) might decay faster than the pure dephasing coupling case ($\theta = \pi/2$) due to the damping effect. As a result of that, in the finite time regime, it is possible to achieve a better charging of QB for the pure dephasing coupling case. However, in the infinite time limit, both cases may achieve the same maximum average energy, given by $\langle E(\infty) \rangle = \Delta/2$. Besides, notice that curves associated to the QB and to the charger are not specular (with respect to the x axis), reflecting the fact that a given amount of energy is also dissipated into the reservoir. When $Al < \Delta\ell$, we find that the charging of the QB performances quite differently compared with that for the $Al > \Delta\ell$ case. Here we can find that although in the infinite charging time limit, both the decoherence coupling ($\theta = 0$) case and the pure dephasing coupling ($\theta = \pi/2$) case may achieve the same maximum average energy, while the decoherence coupling case may reach the maximum earlier than the pure dephasing coupling case. In this regard, the decoherence coupling case seems to be more efficient than the pure dephasing coupling case for charging protocol. Furthermore, we can also find that curves associated to the QB and to the charger are not specular (with respect to the x axis) and the average-energy variation associated to the QB is more than that associated to the charging, reflecting the fact that the QB not only get the energy from the charge, but also can extract the energy from the reservoir. This means that one can extract the energy from the vacuum fluctuations of quantum field in curved spacetime through charging protocol.

3.4 Charging stability

Another important question regards how long a QB can retain a given amount of energy that has been stored during a charging process, in the presence of dissipation. To answer this question, we will inspect the following protocol. At $\tau \geq 0$ we assume the QB is charged by the external charger which has the amplitude A , and this charging process lasts to τ_c . Then we let the charger be switched off, i.e., $A = 0$, for $\tau > \tau_c$. For this kind of protocol, there is in general an energy cost $\delta E_{\text{SW}} = -\langle H_C \rangle$ (evaluated at the time τ_c) associated to the switching operation. Therefore, in a fully quantum case, as noted in Refs. [92, 93], one has to determine whether there is enough energy in the system (the charger) to compensate this additional cost. However, this is not problem in our model, since our QB is charged by a classical source which can be assumed to be big enough to provide the energy required to implement the switch without affecting the performance of the QB. For a closed system, the amount of energy stored in the QB until the time τ_c will remain constant at later times. However, unlike the closed one, a more realistic model—open QB as a result of the interaction with environment will inevitably dissipate part of its energy into the thermal bath. Therefore, it is quite important to quantify the amount of energy retained in the QB, after the charging field has been switched off. To model this protocol, we consider that at $\tau = 0$ the QB is initially prepared in a given ground state. The system then evolves under the action of the charger with amplitude A until the time τ_c . At $\tau = \tau_c$ the reduced

density matrix of the QB is $\tilde{\rho}_{\text{QB}}(\tau_c) = \frac{1}{2}(\mathbf{I} + \vec{\mathbf{r}}(\tau_c) \cdot \vec{\sigma})$ with the state parameters given in (2.13). Correspondingly, the average energy stored in the QB is given by

$$\langle E_{\text{QB}}(\tau_c) \rangle_{\text{DC}} = \frac{\Delta}{2} \left\{ 1 - \frac{\Delta^2}{\Omega^2} e^{-\Gamma_0^r \tau_c} - \frac{\Delta}{\Omega} \left(\frac{e^{\Omega/T} - 1}{e^{\Omega/T} + 1} \right) (1 - e^{-\Gamma_0^r \tau_c}) - \frac{A^2}{\Omega^2} \cos(\Omega \tau_c) e^{-\Gamma_0^r \tau_c} \right\}, \quad (3.22)$$

for the decoherence coupling case, and

$$\langle E_{\text{QB}}(\tau_c) \rangle_{\text{DP}} = \frac{\Delta}{2} \left\{ 1 - \frac{\Delta^2}{\Omega^2} e^{-\Gamma_{\pi/2}^r \tau_c} - \frac{\Delta}{\Omega} \left(\frac{e^{\Omega/T} - 1}{e^{\Omega/T} + 1} \right) (1 - e^{-\Gamma_{\pi/2}^r \tau_c}) - \frac{A^2}{\Omega^2} \cos(\Omega \tau_c) e^{-\Gamma_{\pi/2}^r \tau_c} \right\}, \quad (3.23)$$

for the pure dephasing coupling case, respectively. When $\tau \geq \tau_c$ the charger is switched off (with the amplitude $A = 0$) and therefore this operation may lead to a different dynamics for the QB. In this scenario, the evolution of the QB can also be described with Eq. (2.12) while the state parameters in Eq. (2.13) are different from the $A \neq 0$ case discussed above. Besides, in this case, the effective initial state of the QB can be described in terms of the reduced density matrix $\tilde{\rho}_{\text{QB}}(\tau_c)$. Specifically, as shown in (3.5) the associated parameters for this case can be written as

$$\begin{aligned} \gamma_+ &= \frac{\mu^2}{2} \left(\frac{1}{e^{\Omega/T} + 1} \right) \sum_{n=-\infty}^{n=\infty} \left[P_{-\frac{1}{2} + i \frac{\Omega}{2\pi T}} (\cosh \alpha_n) - \zeta P_{-\frac{1}{2} + i \frac{\Omega}{2\pi T}} (\cosh \beta_n) \right], \\ \gamma_- &= \frac{\mu^2}{2} \left(\frac{1}{e^{-\Omega/T} + 1} \right) \sum_{n=-\infty}^{n=\infty} \left[P_{-\frac{1}{2} - i \frac{\Omega}{2\pi T}} (\cosh \alpha_n) - \zeta P_{-\frac{1}{2} - i \frac{\Omega}{2\pi T}} (\cosh \beta_n) \right], \\ \gamma_z &= 0, \end{aligned} \quad (3.24)$$

for the decoherence coupling case, and

$$\begin{aligned} \gamma_+ &= 0, \quad \gamma_- = 0, \\ \gamma_z &= \frac{\mu^2}{4} \sum_{n=-\infty}^{n=\infty} \left[P_{-\frac{1}{2}} (\cosh \alpha_n) - \zeta P_{-\frac{1}{2}} (\cosh \beta_n) \right], \end{aligned} \quad (3.25)$$

for the pure dephasing case, respectively. Besides, when $\tau > \tau_c$ the evolution of the average energy stored in the QB subjected to external quantum field vacuum fluctuations reads

$$\langle E(\tau) \rangle = \frac{\Delta}{2} \left\{ 1 + \left[\frac{2\langle E_{\text{QB}}(\tau_c) \rangle_{\text{DC}}}{\Delta} - 1 \right] e^{-\Gamma_0^r \tau} - \left(\frac{e^{\Omega/T} - 1}{e^{\Omega/T} + 1} \right) (1 - e^{-\Gamma_0^r \tau}) \right\}, \quad (3.26)$$

for the decoherence coupling case. Here, $\Gamma_0^r = \gamma_+ + \gamma_-$ with γ_{\pm} being in (3.24). For the pure dephasing coupling case, we can find that the average energy stored in the QB after switching off the charging does not change, i.e., $\langle E(\tau) \rangle = \langle E_{\text{QB}}(\tau_c) \rangle_{\text{DP}}$.

In Fig. 12 we show the time evolution of the average energy stored in the QB under this protocol (switching-off the charging ($A = 0$) at time τ_c). We can find that when $A > \Delta$

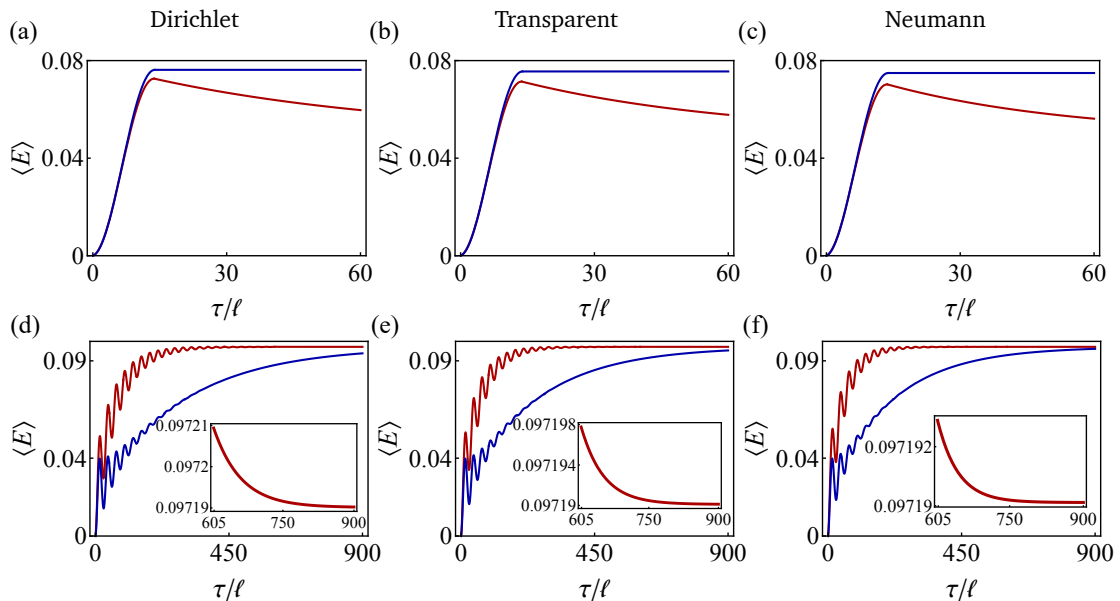


Figure 12. Stability of average energy in the presence of dissipation: (a), (b) and (c) for the $Al = 0.2 > \Delta l = 0.1$ case, while (d), (e), and (f) for the $Al = 0.1 < \Delta l = 0.2$ case. The red curves denote the decoherence coupling case ($\theta = 0$), while the blue curves denote the pure dephasing coupling case ($\theta = \pi/2$). Note that the insets denote the detailed decay for the decoherence coupling case, while the pure dephasing coupling corresponds to the QB effectively decoupled from the external quantum field when the driving field is switched off. Here we have taken the coupling strength $\mu\sqrt{\ell} = 0.2$, the mass $M = 1$, and the relative distance of the QB in BTZ spacetime $r/r_h = 1.001$, respectively.

(Fig. 12 (a), (b), and (c)) for the decoherence coupling case the stored average energy, after the first maximum (at time τ_c) starts to decrease. However, for the pure dephasing coupling case the stored average energy, after the first maximum, presents a flat behaviour, as a result of the effective decoupling of the QB from the external quantum field (resembling the dynamics of a closed system). Besides, we can find the blue curves is above the red ones, which means that more energy can be stored for the pure dephasing coupling case, reflecting a better charging performance compared to the decoherence coupling case. This result is valid for all the three different boundary condition cases. When $A < \Delta$ (Fig. 12 (d), (e), and (f)), we can find that the maximum average energy for both the decoherence coupling and the pure dephasing coupling cases is reached only when the system approaches to its equilibrium state. However, compared with the pure dephasing coupling case the average energy stored in the QB for the decoherence coupling case reaches its equilibrium station earlier. We can choose an appropriate time (also denoted as τ_c) to switch off the driving field, at which the corresponding average energy stored in the QB for the pure decoherence coupling case is high enough, so is almost the same as the maximum one. After this value the stored average energy starts to decrease (seen from the insets), while this degradation is quite trivial. For the pure dephasing coupling case, at that moment (at the chosen τ_c) the average energy stored in the QB would not reach the maximum and is always smaller than that for the decoherence coupling case. This result is valid for all the three different

boundary condition cases. In this regard, when $A < \Delta$ more energy can be stored for the decoherence coupling case in a finite time regime, reflecting a better charging performance compared to the pure dephasing coupling case.

4 Discussions and Conclusions

We find that the dynamics of the average energy stored in the QB quite depends on the weight of the driving amplitude A and the energy-level spacing Δ . This is because that when $A > \Delta$, the driving may plays a dominated role in the dynamical evolution of the QB, while the dissipation due to the coupling to the vacuum fluctuations of quantum field plays a subordinate role. Therefore, oscillatory behavior with slow decay (which may finally leads to an equilibrium state for the QB) is presented. Oscillatory behavior results from the driving, while slow amplitude decay is the consequence of dissipation. However, when $A < \Delta$, this is opposite. the dissipation may plays a dominated role in the dynamical evolution of the QB, while the driving plays a subordinate role. Therefore, the QB will straightly evolve to its equilibrium state while accompanied by decaying small oscillation. Small oscillation is from the driving since the driving is weak, while the decay and dissipative evolution to the equilibrium state result from the dissipation. Therefore, in the charging protocol, one can adjust the strength of the driving to manipulate the charging dynamics.

In summary, we studied how charging performances of a quantum battery, modeled as a two-level system, are influenced by the presence of vacuum fluctuations of a quantum field satisfying the Dirichlet, transparent, and Neumann boundary conditions in the BTZ spacetime. We obtained the analytical dynamics of this QB, and analytically calculated the average energy stored in the QB. We find that when the driving amplitude is stronger/weaker than the energy-level spacing of the QB the pure dephasing dissipative coupling results in better/worse charging performance than the decoherence dissipative coupling case. We also found that compared with the closed QB case, as a result of dissipative coupling the higher Hawking temperature helps to improve the charging performance under certain conditions. This means that it is possible for us to extract energy from vacuum fluctuations in curved spacetime via dissipation in charging protocol. We also considered how different boundary conditions for quantum field affect the charging performance. We found that the boundary condition not only quantitatively but also qualitatively affects the the QB dynamics. It is shown that the maximum average energy stored in the QB increases with the decrease of Hawking temperature for the Dirichlet boundary case, while it is opposite for the transparent and Neumann boundary cases. Furthermore, we also addressed the charging stability by monitoring the energy behaviour after the charging protocol has been switched off. We found that from the perspective of the charging stability, the pure dephasing dissipative coupling may lead to better/worse charging performance than the decoherence dissipative coupling case when the driving amplitude is stronger/weaker than the energy-level spacing of the QB. This result is valid for all the three boundary condition cases. Our study presents a general framework to investigate relaxation effects in curved spacetime, and reveals how spacetime properties and filed boundary condition affect the

charging process. This in turn, from a simple quantum device for the production, storage, and transfer of energy, may shed light on the exploration of the spacetime properties and thermodynamics via the charging protocol.

Acknowledgments

This work was supported by the scientific research start-up funds of Hangzhou Normal University: 4245C50224204016; XL acknowledges the support by the National Natural Science Foundation of China (NSFC) under Grant No. 12065016 and the Discipline-Team of Liupanshui Normal University of China under Grant No. LPSSY2023XKTD11; JJ was supported by NSFC under Grant No. 12035005.

References

- [1] M. A. Nielsen and I. L. Chuang, *Quantum Computation and Quantum Information*, Cambridge university press (2010).
- [2] F. Arute, K. Arya, R. Babbush, D. Bacon, J. C. Bardin, R. Barends et al., *Quantum Supremacy Using a Programmable Superconducting Processor*, *Nature* **574** (2019) 505.
- [3] M. Esposito, U. Harbola and S. Mukamel, *Nonequilibrium Fluctuations, Fluctuation Theorems, and Counting Statistics in Quantum Systems*, *Rev. Mod. Phys.* **81** (2009) 1665.
- [4] M. Campisi, P. Hänggi and P. Talkner, *Colloquium: Quantum Fluctuation Relations: Foundations and Applications*, *Rev. Mod. Phys.* **83** (2011) 771.
- [5] G. T. Landi and M. Paternostro, *Irreversible Entropy Production: From Classical to Quantum*, *Rev. Mod. Phys.* **93** (2021) 035008.
- [6] J. P. Pekola and B. Karimi, *Colloquium: Quantum Heat Transport in Condensed Matter Systems*, *Rev. Mod. Phys.* **93** (2021) 041001.
- [7] R. Alicki and M. Fannes, *Entanglement boost for extractable work from ensembles of quantum batteries*, *Phys. Rev. E* **87** (2013) 042123.
- [8] F. Campaioli, F. A. Pollock and S. Vinjanampathy, *Quantum batteries*, in *Thermodynamics in the Quantum Regime: Fundamental Aspects and New Directions*, F. Binder, L.A. Correa, C. Gogolin, J. Anders and G. Adesso, eds., (Cham), pp. 207–225, Springer International Publishing (2018), DOI.
- [9] F. Campaioli, S. Gherardini, J. Q. Quach, M. Polini and G. M. Andolina, *Colloquium: Quantum Batteries*, *Rev. Mod. Phys.* **96** (2024) 031001.
- [10] F. C. Binder, S. Vinjanampathy, K. Modi and J. Goold, *Quantacell: powerful charging of quantum batteries*, *New Journal of Physics* **17** (2015) 075015.
- [11] G. M. Andolina, M. Keck, A. Mari, M. Campisi, V. Giovannetti and M. Polini, *Extractable Work, the Role of Correlations, and Asymptotic Freedom in Quantum Batteries*, *Phys. Rev. Lett.* **122** (2019) 047702.
- [12] K. V. Hovhannisyanyan, M. Perarnau-Llobet, M. Huber and A. Acín, *Entanglement Generation is Not Necessary for Optimal Work Extraction*, *Phys. Rev. Lett.* **111** (2013) 240401.
- [13] A. E. Allahverdyan, K. V. Hovhannisyanyan, A. V. Melkikh and S. G. Gevorkian, *Carnot Cycle at Finite Power: Attainability of Maximal Efficiency*, *Phys. Rev. Lett.* **111** (2013) 050601.

- [14] X. Yang, Y.-H. Yang, M. Alimuddin, R. Salvia, S.-M. Fei, L.-M. Zhao et al., *Battery Capacity of Energy-Storing Quantum Systems*, *Phys. Rev. Lett.* **131** (2023) 030402.
- [15] H.-L. Shi, S. Ding, Q.-K. Wan, X.-H. Wang and W.-L. Yang, *Entanglement, Coherence, and Extractable Work in Quantum Batteries*, *Phys. Rev. Lett.* **129** (2022) 130602.
- [16] J. Y. Gyhm and U. R. Fischer, *Beneficial and detrimental entanglement for quantum battery charging*, *AVS Quantum Science* **6** (2024) 012001.
- [17] D. Ferraro, M. Campisi, G. M. Andolina, V. Pellegrini and M. Polini, *High-Power Collective Charging of a Solid-State Quantum Battery*, *Phys. Rev. Lett.* **120** (2018) 117702.
- [18] F. Campaioli, F. A. Pollock, F. C. Binder, L. Céleri, J. Goold, S. Vinjanampathy et al., *Enhancing the Charging Power of Quantum Batteries*, *Phys. Rev. Lett.* **118** (2017) 150601.
- [19] J.-Y. Gyhm, D. Šafránek and D. Rosa, *Quantum Charging Advantage Cannot be Extensive without Global Operations*, *Phys. Rev. Lett.* **128** (2022) 140501.
- [20] S. Ghosh, T. Chanda and A. Sen(De), *Enhancement in the performance of a quantum battery by ordered and disordered interactions*, *Phys. Rev. A* **101** (2020) 032115.
- [21] T. F. F. Santos, Y. V. de Almeida and M. F. Santos, *Vacuum-enhanced charging of a quantum battery*, *Phys. Rev. A* **107** (2023) 032203.
- [22] K. Xu, H.-J. Zhu, G.-F. Zhang and W.-M. Liu, *Enhancing the performance of an open quantum battery via environment engineering*, *Phys. Rev. E* **104** (2021) 064143.
- [23] F. H. Kamin, S. Salimi and M. B. Arjmandi, *Steady-state charging of quantum batteries via dissipative ancillas*, *Phys. Rev. A* **109** (2024) 022226.
- [24] F. T. Tabesh, F. H. Kamin and S. Salimi, *Environment-mediated charging process of quantum batteries*, *Phys. Rev. A* **102** (2020) 052223.
- [25] S. Seah, M. Perarnau-Llobet, G. Haack, N. Brunner and S. Nimmrichter, *Quantum Speed-up in Collisional Battery Charging*, *Phys. Rev. Lett.* **127** (2021) 100601.
- [26] R. Salvia, M. Perarnau-Llobet, G. Haack, N. Brunner and S. Nimmrichter, *Quantum advantage in charging cavity and spin batteries by repeated interactions*, *Phys. Rev. Res.* **5** (2023) 013155.
- [27] D. Rossini, G. M. Andolina, D. Rosa, M. Carrega and M. Polini, *Quantum Advantage in the Charging Process of Sachdev-Ye-Kitaev Batteries*, *Phys. Rev. Lett.* **125** (2020) 236402.
- [28] D. Rosa, D. Rossini, G. M. Andolina, M. Polini and M. Carrega, *Ultra-stable charging of fast-scrambling SYK quantum batteries*, *Journal of High Energy Physics* **2020** (2020) 67.
- [29] D. Qu, X. Zhan, H. Lin and P. Xue, *Experimental optimization of charging quantum batteries through a catalyst system*, *Phys. Rev. B* **108** (2023) L180301.
- [30] G. Zhu, Y. Chen, Y. Hasegawa and P. Xue, *Charging Quantum Batteries via Indefinite Causal Order: Theory and Experiment*, *Phys. Rev. Lett.* **131** (2023) 240401.
- [31] C.-K. Hu, J. Qiu, P. J. P. Souza, J. Yuan, Y. Zhou, L. Zhang et al., *Optimal charging of a superconducting quantum battery*, *Quantum Science and Technology* **7** (2022) 045018.
- [32] J. Joshi and T. S. Mahesh, *Experimental investigation of a quantum battery using star-topology nmr spin systems*, *Phys. Rev. A* **106** (2022) 042601.
- [33] G. Gemme, M. Grossi, D. Ferraro, S. Vallecorsa and M. Sassetti, *IBM quantum platforms: A quantum battery perspective*, *Batteries* **8** (2022) .

- [34] D. Farina, G. M. Andolina, A. Mari, M. Polini and V. Giovannetti, *Charger-mediated energy transfer for quantum batteries: An open-system approach*, *Phys. Rev. B* **99** (2019) 035421.
- [35] S.-Y. Bai and J.-H. An, *Floquet engineering to reactivate a dissipative quantum battery*, *Phys. Rev. A* **102** (2020) 060201.
- [36] F. Zhao, F.-Q. Dou and Q. Zhao, *Quantum battery of interacting spins with environmental noise*, *Phys. Rev. A* **103** (2021) 033715.
- [37] M. Carrega, A. Crescente, D. Ferraro and M. Sassetti, *Dissipative dynamics of an open quantum battery*, *New Journal of Physics* **22** (2020) 083085.
- [38] F. Barra, *Dissipative Charging of a Quantum Battery*, *Phys. Rev. Lett.* **122** (2019) 210601.
- [39] Y. Yao and X. Q. Shao, *Stable charging of a Rydberg quantum battery in an open system*, *Phys. Rev. E* **104** (2021) 044116.
- [40] S. Ghosh, T. Chanda, S. Mal and A. Sen(De), *Fast charging of a quantum battery assisted by noise*, *Phys. Rev. A* **104** (2021) 032207.
- [41] H.-P. Breuer and F. Petruccione, *The Theory of Open Quantum Systems*, Oxford University Press, USA (2002).
- [42] D. Manzano, *A short introduction to the Lindblad master equation*, *AIP Advances* **10** (2020) 025106
[https://pubs.aip.org/aip/adv/article-pdf/doi/10.1063/1.5115323/12881278/025106.1_online.pdf].
- [43] F. Benatti, R. Floreanini and M. Piani, *Environment Induced Entanglement in Markovian Dissipative Dynamics*, *Phys. Rev. Lett.* **91** (2003) 070402.
- [44] F. Benatti and R. Floreanini, *Entanglement generation in uniformly accelerating atoms: Reexamination of the Unruh effect*, *Phys. Rev. A* **70** (2004) 012112.
- [45] M. S. Soares, N. F. Svaiter and G. Menezes, *Entanglement dynamics: Generalized master equation for uniformly accelerated two-level systems*, *Phys. Rev. A* **106** (2022) 062440.
- [46] H. Yu and J. Zhang, *Understanding Hawking radiation in the framework of open quantum systems*, *Phys. Rev. D* **77** (2008) 024031.
- [47] H. Yu, *Open Quantum System Approach to the Gibbons-Hawking Effect of de Sitter Space-time*, *Phys. Rev. Lett.* **106** (2011) 061101.
- [48] G. Kaplanek and C. P. Burgess, *Hot cosmic qubits: late-time de Sitter evolution and critical slowing down*, *Journal of High Energy Physics* **2020** (2020) 53.
- [49] G. Kaplanek and E. Tjoa, *Effective master equations for two accelerated qubits*, *Phys. Rev. A* **107** (2023) 012208.
- [50] J. Hu and H. Yu, *Geometric phase for an accelerated two-level atom and the Unruh effect*, *Phys. Rev. A* **85** (2012) 032105.
- [51] Z. Tian and J. Jing, *Geometric phase of two-level atoms and thermal nature of de Sitter spacetime*, *Journal of High Energy Physics* **2013** (2013) 109.
- [52] X. Liu, Z. Tian and J. Jing, *Entanglement dynamics in κ -deformed spacetime*, *Science China Physics, Mechanics & Astronomy* **67** (2024) 100411.
- [53] H. Du and R. B. Mann, *Fisher information as a probe of spacetime structure: relativistic quantum metrology in (A)dS*, *Journal of High Energy Physics* **2021** (2021) 112.

- [54] Z. Tian, J. Wang, H. Fan and J. Jing, *Relativistic quantum metrology in open system dynamics*, *Scientific Reports* **5** (2015) 7946.
- [55] J. Feng and J.-J. Zhang, *Quantum Fisher information as a probe for Unruh thermality*, *Physics Letters B* **827** (2022) 136992.
- [56] E. Patterson and R. B. Mann, *Fisher information of a black hole spacetime*, *Journal of High Energy Physics* **2023** (2023) 214.
- [57] J. Q. Quach, T. C. Ralph and W. J. Munro, *Berry Phase from the Entanglement of Future and Past Light Cones: Detecting the Timelike Unruh Effect*, *Phys. Rev. Lett.* **129** (2022) 160401.
- [58] Z. Tian and J. Jing, *Using nanokelvin quantum thermometry to detect timelike Unruh effect in a bose-einstein condensate*, *The European Physical Journal C* **83** (2023) 1022.
- [59] Z. Tian, J. Jing and J. Du, *Direct characteristic-function tomography of the quantum states of quantum fields*, *Science China Physics, Mechanics & Astronomy* **66** (2023) 110412.
- [60] A. Teixidó-Bonfill, A. Ortega and E. Martín-Martínez, *First law of quantum field thermodynamics*, *Phys. Rev. A* **102** (2020) 052219.
- [61] A. Ortega, E. McKay, A. M. Alhambra and E. Martín-Martínez, *Work Distributions on Quantum Fields*, *Phys. Rev. Lett.* **122** (2019) 240604.
- [62] J. Foo, S. Onoe, R. B. Mann and M. Zych, *Thermality, causality, and the quantum-controlled unruh-dewitt detector*, *Phys. Rev. Res.* **3** (2021) 043056.
- [63] J. Foo, C. S. Arabaci, M. Zych and R. B. Mann, *Quantum Signatures of Black Hole Mass Superpositions*, *Phys. Rev. Lett.* **129** (2022) 181301.
- [64] L. C. Barbado, E. Castro-Ruiz, L. Apadula and Časlav. Brukner, *Unruh effect for detectors in superposition of accelerations*, *Phys. Rev. D* **102** (2020) 045002.
- [65] E. Martín-Martínez and T. R. Perche, *What gravity mediated entanglement can really tell us about quantum gravity*, *Phys. Rev. D* **108** (2023) L101702.
- [66] L. J. Henderson, A. Belenchia, E. Castro-Ruiz, C. Budroni, M. Zych, Časlav. Brukner et al., *Quantum Temporal Superposition: The Case of Quantum Field Theory*, *Phys. Rev. Lett.* **125** (2020) 131602.
- [67] J. Clarke and F. K. Wilhelm, *Superconducting quantum bits*, *Nature* **453** (2008) 1031.
- [68] P. J. Leek, J. M. Fink, A. Blais, R. Bianchetti, M. Göppl, J. M. Gambetta et al., *Observation of Berry's Phase in a Solid-state Qubit*, *Science* **318** (2007) 1889 [<https://www.science.org/doi/pdf/10.1126/science.1149858>].
- [69] C. Monroe, W. C. Campbell, L.-M. Duan, Z.-X. Gong, A. V. Gorshkov, P. W. Hess et al., *Programmable Quantum Simulations of Spin Systems with Trapped ions*, *Rev. Mod. Phys.* **93** (2021) 025001.
- [70] D. Guéry-Odelin, A. Ruschhaupt, A. Kiely, E. Torrontegui, S. Martínez-Garaot and J. G. Muga, *Shortcuts to Adiabaticity: Concepts, Methods, and Applications*, *Rev. Mod. Phys.* **91** (2019) 045001.
- [71] M. Bañados, C. Teitelboim and J. Zanelli, *Black Hole in Three-dimensional Spacetime*, *Phys. Rev. Lett.* **69** (1992) 1849.
- [72] S. Deser, R. Jackiw and G. 't Hooft, *Three-dimensional Einstein gravity: Dynamics of flat space*, *Annals of Physics* **152** (1984) 220.

- [73] S. Deser and R. Jackiw, *Classical and quantum scattering on a cone*, *Communications in Mathematical Physics* **118** (1988) 495.
- [74] G. Lifschytz and M. Ortiz, *Scalar field quantization on the (2+1)-dimensional black hole background*, *Phys. Rev. D* **49** (1994) 1929.
- [75] S. Carlip, *The (2+ 1)-dimensional black hole*, *Classical and Quantum Gravity* **12** (1995) 2853.
- [76] D. Binosi, V. Moretti, L. Vanzo and S. Zerbini, *Quantum scalar field on the massless (2 + 1)-dimensional black hole background*, *Phys. Rev. D* **59** (1999) 104017.
- [77] L. Hodgkinson and J. Louko, *Static, stationary, and inertial Unruh-Dewitt detectors on the BTZ black hole*, *Phys. Rev. D* **86** (2012) 064031.
- [78] B. Pourhassan, M. Faizal, Z. Zaz and A. Bhat, *Quantum fluctuations of a BTZ black hole in massive gravity*, *Physics Letters B* **773** (2017) 325.
- [79] L. J. Henderson, R. A. Hennigar, R. B. Mann, A. R. H. Smith and J. Zhang, *Harvesting entanglement from the black hole vacuum*, *Classical and Quantum Gravity* **35** (2018) 21LT02.
- [80] K. Bueley, L. Huang, K. Gallock-Yoshimura and R. B. Mann, *Harvesting mutual information from BTZ black hole spacetime*, *Phys. Rev. D* **106** (2022) 025010.
- [81] L. de Souza Campos and C. Dappiaggi, *The anti-Hawking effect on a BTZ black hole with Robin boundary conditions*, *Physics Letters B* **816** (2021) 136198.
- [82] L. J. Henderson, R. A. Hennigar, R. B. Mann, A. R. Smith and J. Zhang, *Anti-Hawking phenomena*, *Physics Letters B* **809** (2020) 135732.
- [83] M. P. G. Robbins and R. B. Mann, *Anti-Hawking phenomena around a rotating BTZ black hole*, *Phys. Rev. D* **106** (2022) 045018.
- [84] Y. Yu, J. Zhang and H. Yu, *The Lamb shift in the BTZ spacetime*, *Journal of High Energy Physics* **2023** (2023) 209.
- [85] R. Emparan, A. M. Frassino, M. Sasieta and M. Tomašević, *Holographic complexity of quantum black holes*, *Journal of High Energy Physics* **2022** (2022) 204.
- [86] S. Carlip, *The (2 + 1)-dimensional black hole*, *Classical and Quantum Gravity* **12** (1995) 2853.
- [87] H. Geng, *Open Ads/CFT via a double-trace deformation*, *Journal of High Energy Physics* **2024** (2024) 12.
- [88] S. J. Avis, C. J. Isham and D. Storey, *Quantum field theory in anti-de Sitter space-time*, *Phys. Rev. D* **18** (1978) 3565.
- [89] *8 - special functions*, in *Table of Integrals, Series, and Products (Eighth Edition)*, D. Zwillinger, V. Moll, I. Gradshteyn and I. Ryzhik, eds., (Boston), pp. 867–1013, Academic Press (2015), DOI.
- [90] D. Jennings, *On the response of a particle detector in anti-de Sitter spacetime*, *Classical and Quantum Gravity* **27** (2010) 205005.
- [91] A. Crescente, M. Carrega, M. Sassetti and D. Ferraro, *Charging and energy fluctuations of a driven quantum battery*, *New Journal of Physics* **22** (2020) 063057.
- [92] G. M. Andolina, D. Farina, A. Mari, V. Pellegrini, V. Giovannetti and M. Polini,

Charger-mediated energy transfer in exactly solvable models for quantum batteries, *Phys. Rev. B* **98** (2018) 205423.

- [93] W. J. Chetcuti, C. Sanavio, S. Lorenzo and T. J. G. Apollaro, *Perturbative many-body transfer*, *New Journal of Physics* **22** (2020) 033030.